Doctoral Dissertation

Bacterial cellulose-based functional composites with enhanced mechanical properties

バクテリアセルロースを基盤とした

高強度機能性複合材料の開発

Qidong Wang

July 2018

Graduate School of Engineering

Osaka University

Contents

Chapter 3

Facile preparation of a novel transparent composite film based on bacterial cellulose and atactic polypropylene

General Introduction

Nowadays, due to the continuous depletion of fossil fuels and various environment issues, it becomes an emergent task for researchers to find environmental-friendly and sustainable materials for scientific research and industrial production. Renewable bio-materials that can be used for both bioenergy and bioproducts are a possible alternative to common petroleum-based and synthetic products.

During the past few decades, various types of bio-materials have been investigated, among which cellulose is a very important and fascinating biopolymer. As an almost inexhaustible natural polymeric raw material, cellulose is of special importance both in daily lives and in industries to replace non-renewable resources[1-4]. After firstly described in 1838 by the French chemist Anselme Payen[5], the interdisciplinary research and utilization of this abundant natural polymer have become a hot topic for applications in science, medicine and technology[6].

Formed by repeated connection of glucose building blocks, cellulose possesses plenty of hydroxyl groups forming abundant inter- and intra-molecular hydrogen bonds

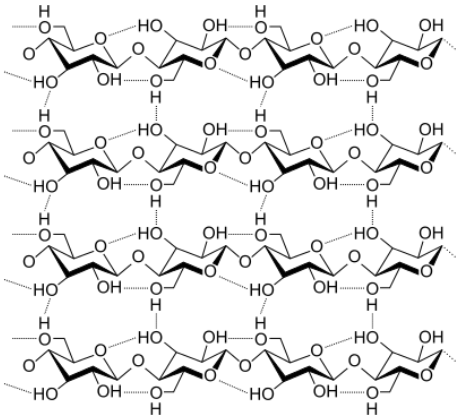

Figure 1. Molecular structure of cellulose with intra- and inter-chain hydrogen bonds.

(shown in Figure 1), which leads to its hydrophilicity, chirality, biodegradability, and broad chemical-modifying capacity[7]. Therefore, it shows promising potentials to prepare functional materials which can be used in foods, paper making, clothes and cosmetic industries. Cellulose can be isolated and purified from plant sources such as cotton, wood and algae through various physical, chemical, and enzymatic methods. However, residues such as hemicellulose, lignin, pectin and other substances are hard to remove, which results in the low purity of cellulose. As a result, the application of cellulose in bio-medical field is greatly limited.

Bacterial cellulose (BC), a special natural cellulose, can be facilely synthesized by certain bacteria such as *Gluconacetobacter xylinus*[6] and conditions commonly used are shown in Figure 2. Through the alteration of cultivation conditions during fermentation, the shape and supermolecular structure of BC pellicles are able to be controlled, which would further influence the properties of BC. Compared to the widely used plant-derived cellulose, BC pellicles enjoys its distinguishing advantages such as high purity, high porosity and high water content (up to 99%)[8-10]. Along with good biodegradability and biocompatibility, BC becomes an ideal choice in biomedical and biotechnological fields. It's potential applications are wound dressing, tissue

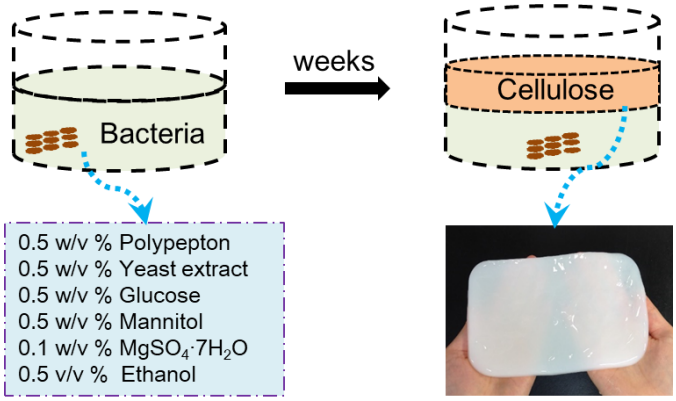

Figure 2. The illustration of biofabrication process of BC pellicle.

regeneration, skin substitutes[11-14] and drug delivery system[15,16]. Besides the applications in biomedical area, dried BC film is also utilized as diaphragms for loudspeakers[17], food packaging films[18], and vulnerable historic silk fabrics reinforcement for storage and display[19].

Originated from the unique three-dimensional (3D) network structure and a high crystallinity up to 84-89%[20], BC exhibits its satisfactory mechanical properties. The typical Young's modulus of BC pellicles reaches 15-35 GPa, with a tensile strength in the range of 200-300 MPa[21] (2~3 times of that of cellulose), making it a promising choice to enhance other materials which require superior physical strength and stability. On the other hand, the presence of numerous pores reduces the stress bearing capability and elasticity of BC sheets.

Despite its good features, pristine BC lacks certain functional properties, which restricts its applications in various fields. For example, BC hydrogel with a high water content is an excellent wound dressing material which accelerates the healing process[22]. However, it is short of antimicrobial and antioxidative properties to prevent infection, which are also important for wound healing. Besides, like other common cellulose materials, neat BC sheet (wet or dried state) also lacks stimuli-sensitivity, electrical conductivity, hydrophobicity, and optical transparence. As a consequence, its applications in sensors, batteries, electrical/optoelectronic devices or oil/water separation are limited[23,24].

In order to address the limitations of BC mentioned above, synthesis of BC-based functional composites has been conducted, utilizing its superior network structure and high mechanical properties. BC plays a role as matrix or reinforcement material in these composite materials. In some researches, BC sheets are homogenized

into cellulose paste or ground into cellulose powders for better reaction and composition with other components, which undoubtfully breaks the network structure of BC and influence its physical strength. Hence, to fully take advantage of the excellent mechanical properties of BC, integral BC pellicles would be directly used for the preparation of BC-based functional composites in this doctoral thesis.

Commonly, two approaches are utilized for BC composites synthesis. For the first method, reinforcement materials are added into the culture media at the start of the static BC synthetic process. The schematic illustration of this strategy is shown in Figure 3. During the formation of BC pellicles, the added materials are trapped in the BC fibril network[25], resulting in a stable BC composite. By this method, several BC-based composites have been successfully prepared. For instance, through the addition of carbon nanotubes (CNTs) into the culture media, a BC/CNTs composite with enhanced physico-mechanical properties was fabricated[26]. Similarly, BC/aloe vera composite films were obtained by adding aloe vera into the synthetic media of BC[27]. This method has two major deficiencies. During the static culture of BC, the reinforcement materials may precipitate or move lower in the media whereas the BC sheet only forms at the media/air interface, leading to an inhomogeneous BC composite. On the other hand, the materials added to the media may be toxic for the microorganism,

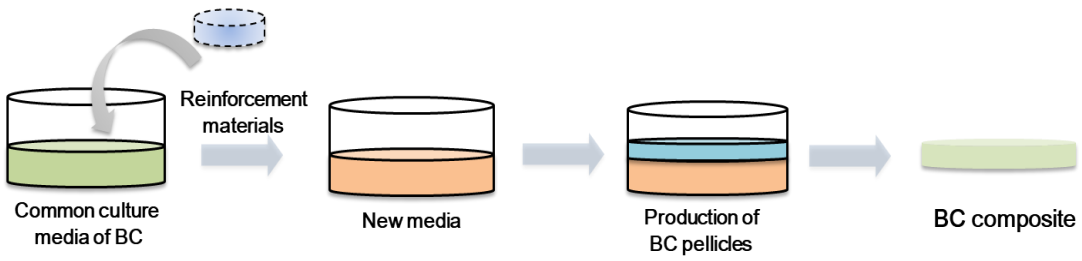

Figure 3. Illustration of BC composites synthesized by adding materials during the static culture of BC pellicles.

which would have great influence on the formation and structure of BC.

BC-based composites can also be fabricated by incorporating nano-particles (NPs), liquids and various solutions into the porous structure of obtained BC sheet (Figure 4), preserving the good structural integrity and mechanical characteristics of BC. There are three types of interactions between BC nanofibers and the reinforcement materials. The NPs and liquids can penetrate into the porous BC matrix and be physically absorbed by the BC fibers. BC/Ag composite was synthesized in this way to achieve antibacterial activities[28]. Owing to the abundant OH moieties on the BC chains, it becomes very easy for BC nanofibers to form hydrogen bonds with the invading materials. Thus BC/Hydroxylapatite composite was obtained to enlarge the biomedical application of BC[29]. In addition to the aforementioned physical absorbance and hydrogen bonding, researchers usually prepare BC-based functional composites by forming interpenetrating network (IPN) between BC and other polymers. Without any chemical bond, the two networks entangle with each other and cannot be pulled apart. By this mean, BC/polyacrylamide gels able to sustain not only high elongation but also high compression have been synthesized[30]. The main obstacle for the second composite production strategy lies in the size and nature of the penetrating materials. Evidently, large particles cannot impregnate into the pores of BC nanofiber network. Meanwhile, it's not easy for hydrophobic materials to combine with BC. However, in comparison to

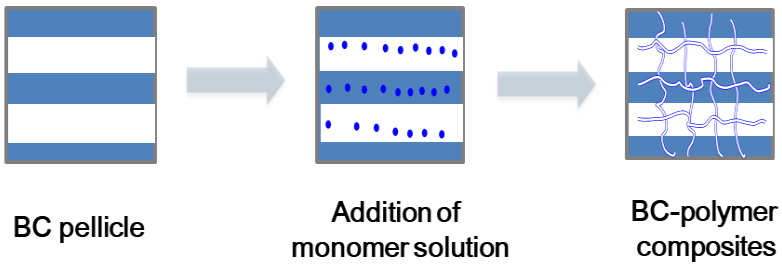

Figure 4. Preparation of BC composites with porous BC pellicles.

the first method which obtains composite directly through the static cultivation of BC, the second method discussed here shows more advantages such as facile preparation, uniform structure, superior mechanical strength and controllable properties. Therefore, the second method is adopted for this research.

Novel multifunctional BC composites with attractive performances have been fabricated through the functionalization of BC with inorganic or organic materials. These two main classes can be further divided into BC composites with metals, metal oxides and polymers. The detailed classifications with specific examples are exhibited in Figure 5. Utilizing BC as a matrix, the preparation of BC-based composites gathers together excellent properties of BC with the ones displayed by typical inorganic or organic materials like antibacterial, catalytic, photocatalytic, magnetic, conductive properties, as well as biomedical and transparent activity[6].

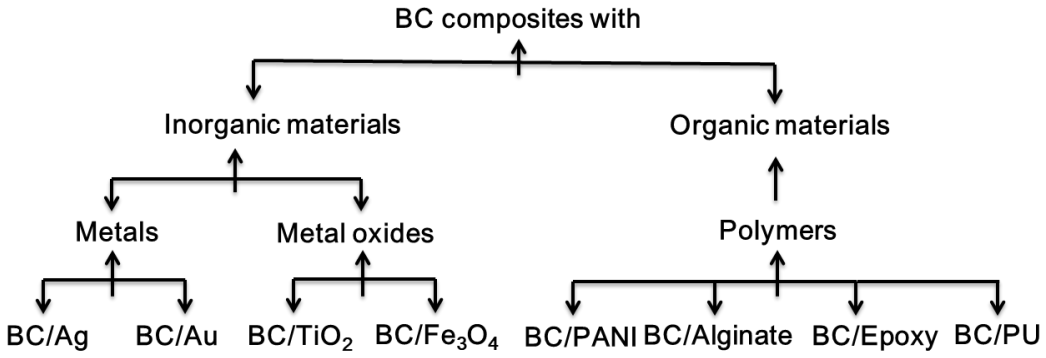

Figure 5. A generalized classification of BC-based functional composites with inorganic and organic materials.

Metals and metal oxides, due to their small size, charged nature and individual behaviors, are promising to form composites with polymeric matrix. By incorporating these inorganic particles into polymer materials, the resulting composites acquire prominent features such as antimicrobial property, catalytic and photo-oxidizing activities，and magnetic capability. Similarly, BC pellicles, with excellent porous

network structure, can be used to make composites with metals and metal oxides *via* various synthetic approaches (as shown in Figure 6). BC/Ag nanocomposite was prepared by impregnating BC pellicles into $AgNO_3$ solution, which was reduced by $NaBH_4$ to produce Ag nanoparticles thereafter[31]. The obtained BC/Ag composite exhibited strong antibacterial effects against different types of bacterial species, which had the potential application for wound dressing. As a promising support as well as reducing agent, amidoxime surface functionalized BC was used to synthesize gold particles that distributed homogeneously on BC fibers surface[32]. With high catalytic activity and desired stability, the present BC/Au composite showed promising applications in organic industry. In addition to metals, a few metal oxides are also investigated to combine with BC to enhance its functional properties. Photocatalytic mesoporous BC/TiO_2 composite was fabricated by immobilizing TiO_2 to oxidized BC to produce a novel material[33]. The BC/TiO_2 membrane possessed better pH, temperature stability, and reusability, which showed combined photocatalytic and biocatalytic degradation of textile dye. Magnetically responsive BC sheets containing Fe_3O_4 nanoparticles were prepared by in situ co-precipitation method without oxygen[34]. Through further modification by fluoroalkyl silane, the hydrophobic and lipophobic BC/Fe_3O_4 composite membrane would have potential applications in electronic actuators, magnetographic printing, and information storage.

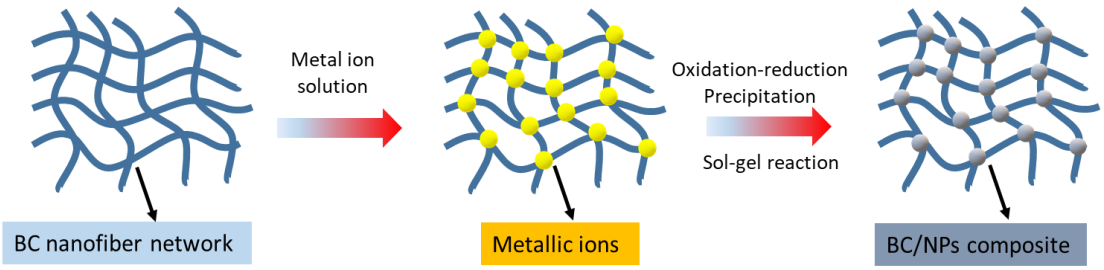

Figure 6. Schematic diagram of the preparation of BC/metal NPs composite.

Compared with the aforementioned inorganic materials, polymers are organic in nature, and most of them have adequate hydrogen bonding sites. The similarities between BC and polymeric materials facilitate the researches on BC/polymer composites, which usually have uniform structure and considerable stability. According to specific purposes, numerous BC composites with polymers have been prepared aiming at improvement in conducting capacities, biomedical applications, mechanical and optical properties of BC. Recently, conductive polymer polyaniline (PANI) has been intensively studied for the preparation of BC/PANI composite. BC/PANI composite membranes were fabricated by oxidative polymerization of aniline with ammonium persulfate as an oxidant[35] (Figure 7). Combing the electronic characteristics of PANI and outstanding mechanical properties of BC, the obtained nanocomposites could be applied in electrodes and other electronic devices. To expand applications of BC in biomedical fields, a novel BC/Alginate composite scaffold was fabricated by freeze drying and subsequent crosslinking with Ca^{2+} [36]. Because of its biocompatibility and open macroporous structure, the BC/Alginate composite could potentially be used as a scaffold for tissue engineering. With high tensile strength and low coefficient of thermal expansion (CTE), BC film has been applied as flexible substrate for displays and optoelectronic devices. However, the transparency of BC film in the visible range is not satisfactory. A transparent BC/epoxy composite was fabricated at a fiber content as high

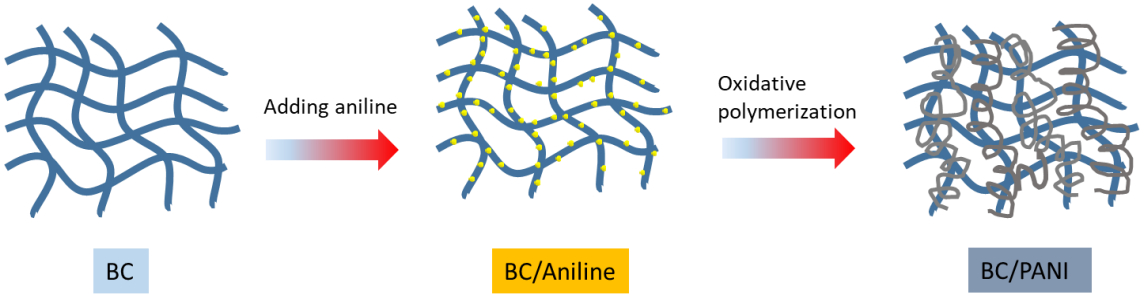

Figure 7. Schematic diagram of the preparation of BC/PANI composite.

as 70%, which maintained the flexibility and ductility of the plastic resin as well as the low CTE and superior physical strength of BC film[37]. Nanocomposite film of BC and polyurethane (PU) based resin was also prepared and utilized as a substrate for flexible displays. The obtained BC/PU composite film showed high transparency along with good thermal stability, which is a promising material for the development of substrate for flexible organic light emitting diodes (OLEDs) display.

Considering the benefits and drawbacks of BC and inorganic/organic reinforcement materials, it seems that it is more facile and valuable to prepare BC/polymer functional composites for practical biomedical and industrial applications. Herein, three types of polymeric materials whose mechanical properties are in urgent need of enhancement are focused and discussed.

Hydrogels are a class of soft materials composed of three-dimensionally (3D) cross-linked polymer networks that accommodate an abundance of water[38]. With features similar to those of biological issues, hydrogels are expected to find various biomedical applications. However, due to their water-rich porous structure, the weak mechanical properties bring hindrance to the wide utilization of hydrogels. Moreover, synthetic hydrogels are usually composed of randomly oriented isotropic networks whereas biological systems adopt anisotropic structures with hierarchically building units, as represented by muscles[39], skin[40], and articular cartilage[41]. The difference between isotropic hydrogel and anisotropic hydrogel was shown in Figure 8. Considering the essential role of anisotropy in biological system, it's reasonable to develop anisotropic hydrogels for exploring biomimetic applications. On the other hand, BC pellicle acts as ideal reinforcing element in polymer matrix. Through static culture of certain bacteria, BC hydrogel with anisotropic structure can be prepared[17,42].

Therefore, it's possible to fabricate anisotropic BC/polymer composite hydrogels which combine the advantages of BC and polymer hydrogels.

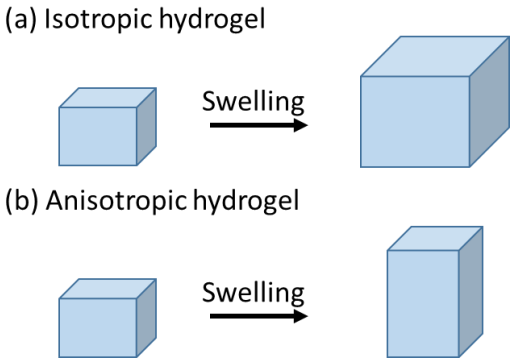

Figure 8. Size change of (a) isotropic hydrogel and (b) anisotropic hydrogel upon swelling.

Aerogels refer to one class of highly interconnected porous and lightweight solid materials formed by replacing the liquid in a gel by air[43], in which supercritical CO_2 drying and freeze-drying techniques are often used. The most noticeable characteristics of aerogels include low thermal conductivity, flexibility, low weight, high porosity and large surface area. Among the three aerogel categories based on the composition, polymeric silica aerogels (SAs) made from the hydrolysis condensation of organosilicon compounds such as alkyltrialkoxysilane and tetraethoxysilane (TEOS) are most studied. The high porosity, low density as well as hydrophobicity enable the SAs to display promising potentials as an ideal oil sorbent candidate, whereas the inherent fragility and comparatively high cost have restricted the wide applications of SAs. In this aspect, the excellent network structure of BC aerogel can provide support for SAs, resulting in a BC/SAs composite aerogel with enhanced mechanical properties and stability.

Transparent polymer films have gained tremendous interest due to their varied applications in electronics, optoelectronics as well as food and packaging industries[44].

For instance, films made from polyethylene (PE), poly(vinyl chloride) (PVC) and poly(vinylidene chloride) (PVDC) are widely used in our daily life and industrial production. The main problems of thermoplastic films lie in their poor heat resistance and low mechanical properties. BC film is an excellent reinforcement material for the above transparent polymer films due to its chemical stability, good mechanical strength, relative thermo-stabilization, and alterable optical transparency.

Based on the background described above, this doctoral thesis focuses on the preparation of BC-based functional composites with enhanced mechanical properties. This thesis contains 3 chapters (as shown in Figure 9).

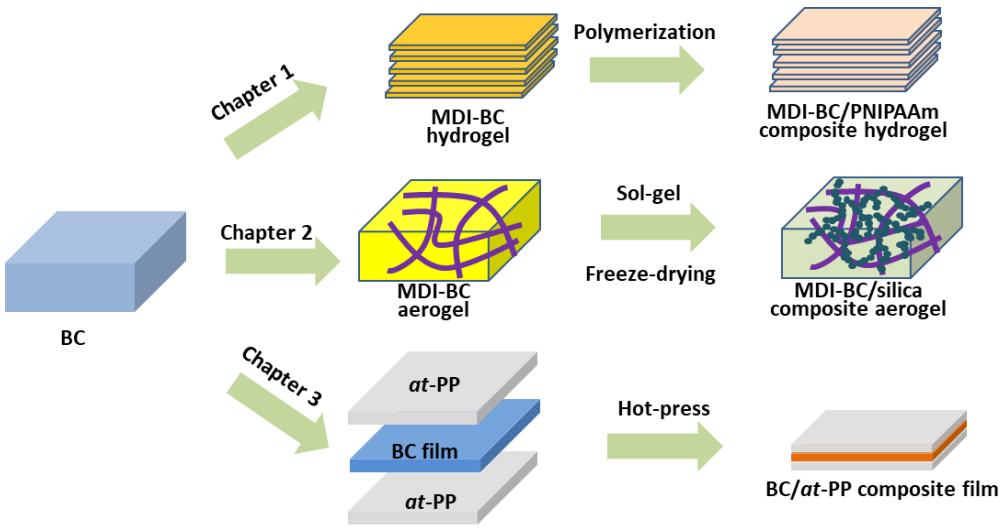

Figure 9. A general summary of the three chapters for the preparation of BC-based functional composites.

Contents of this thesis

Chapter 1

This chapter deals with the unique morphology and properties of methylene diphenyl diisocyanate (MDI)-modified bacterial cellulose/poly(*N*-isopropylacrylamide) (BC/PNIPAAm) composite hydrogel prepared by in situ polymerization method. The influence of the molar ratio of MDI/glucose unit of BC on the properties of the resulting hydrogel was investigated. After the MDI modification, the BC/PNIPAAm composite hydrogel could preserve the unique layered (known as anisotropic) structure, which led to the anisotropic thermo-sensitive property. The mechanical property and responsive rate to temperature change of the obtained composite hydrogels were also carefully discussed.

Chapter 2

Methylene diphenyl diisocyanate (MDI)-modified bacterial cellulose (BC)/silica composite aerogel was prepared by a facile sol-gel process followed by freeze-drying. Pristine BC aerogel and BC/silica aerogel without modification were also fabricated for comparison with MDI-BC/silica aerogel. The influence of the presence of BC matrix as well as MDI modification on the mechanical properties was studied focusing on the compressive strength and shape-recovery capability. Furthermore, the oil absorption ability and recyclability of the obtained composite aerogels were also investigated. The present hydrophobic MDI-BC/silica aerogel with reinforced physical properties has potential as oil sorbent for oil/water separation.

Chapter 3

A facile and cost-effective method was developed to prepare transparent bacterial cellulose/atactic polypropylene (BC/*at*-PP) composite film by a simple "sandwich" hot-press process. With a typical three-layered structure wherein one BC layer was sandwiched between two layers of *at*-PP resin, the present composite film exhibited good hydrophobicity. The effect of combination between BC and *at*-PP was studied to reveal the changes in transparency and mechanical properties of the composite film. Based on the good features, the BC/*at*-PP composite film holds tremendous potential as transparent film for food packaging and optoelectronics applications.

References

1. R. J. Moon, A. Martini, J. Nairn, J. Simonsen, J. Youngblood, *Chem. Soc. Rev.*, 2011,**40**, 3941-3994.
2. X. Qiu, S. Hu, *Materials*, 2013, **6**, 738-781.
3. D. Klemm, B. Heublein, H. P. Fink, A. Bohn, *Angew. Chem. Int. Ed.*, 2005, **44**, 3358-3393.
4. D. Klemm, F. Kramer, S. Moritz, T. Lindström, M. Ankerfors, D. Gray, A. Dorris, *Angew. Chem. Int. Ed.*, 2011, **50**, 5438-5466.
5. A. Payen, C. R. Hebd, *Seances Acad. Sci.*, 1838, **7**, 1052-1056.
6. W. Hu, S. Chen, J. Yang, Z. Li, H. Wang, *Carbohyd. Polym.*, 2014, **101**, 1043-1060.
7. D. Klemm, B. Heublein, H. P. Fink, A. Bohn, *Angew. Chem. Int. Edit.*, 2005, **44(22)**, 3358-3393.
8. Y. Huang, C.L. Zhu, J.Z. Yang, Y. Nie, C.T. Chen and D.P. Sun, *Cellulose*, 2014, **21(1)**, 1-30.
9. N. Shah, M. Ul-Islam, W.A. Khattak, and J.K. Park, *Carbohyd. Polym.*, 2013, **98(2)**, 1585-1598.
10. Y. Kurimoto, M. Takeda, A. Koizumi, S. Yamauchi, S. Doi, Y. Tamura, *Bioresour. Technol.*, 2000, **74**, 151-157.
11. D. Ciechańska, Fibres. *Text. East. Eur.*, 2004, **12(4)**, 69-72.
12. W. Czaja, A. Krystynowicz, S. Bielecki and R.M. Brown, *Biomaterials*, 2006, **27(2)**, 145-151.
13. W. Czaja, D.J. Young, M. Kawecki and R.M. Brown, *Biomacromolecules*, 2007, **8(1)**, 1-12.
14. N. Petersen, P. Gatenholm, *Appl. Microbiol. Biot.*, 2011, **91(5)**, 1277-1286.
15. M.C.I.M. Amin, N. Ahmad, N. Halib and I. Ahmad, *Carbohyd. Polym.*, 2012, **88(2)**, 465-473.
16. E. Trovatti, C.S.R. Freire, P.C. Pinto, I.F. Almeida, P.Costa, A.J.D. Silvestre, C.P.

Neto, C. Rosado, *Int. J. Pharm.*, 2012, **435(1)**, 83-87.

17. M. Iguchi, S. Yamanaka, A. Budhiono, *J. Mater. Sci.*, 2000, **35(2)**, 261-270.
18. P. Wanichapichart, W. Taweepreeda, S. Nawae, P. Choomgan, D. Yasenchak, *Radiat, Phys. Chem.*, 2012, **81(8)**, 949-953.
19. S. Wu, M. Li, B. Fang, H. Tong, *Carbohyd. Polym.*, 2012, **88(2)**, 496-501
20. W. Czaja, D. Romanovicz, R. Malcolm Brown, *Cellulose*, 2004, **11(3-4)**, 403-411
21. R.M. Brown, J. Willison, C.L. Richardson, *Proc. Natl. Acad. Sci.*, 1976, **73(12)**, 4565-4569
22. O. Shezad, S. Khan, T. Khan, J.K. Park, *Carbohyd. Polym.*, 2010, **82**, 173-180.
23. B.R. Evans, H.M. O'Neill, V.P. Malyvanh, I. Lee, J. Woodward, *Biosens. Bioelectron.*, 2003, **8**, 917-923.
24. Z. Shi, S. Zang, F. Jiang, L. Huang, D. Lu, Y. Ma, G. Yang, *RSC Adv.*, 2012, **2**, 1040-1046
25. M. Ul-Islam, T. Khan, J.K. Park, *Carbohyd. Polym.*, 2012, **88(2)**, 596-603.
26. Z. Yan, S. Chen, H. Wang, B. Wang, J. Jiang, *Carbohyd. Polym.*, 2008, **74**, 659-665.
27. O. Saibuatong, M. Philsalaphong, *Carbohyd. Polym.*, 2010, **79**, 455-460.
28. L.C de Santa Maria, A.L. Santos, P.C. Oliveira, H.S. Barud, Y. Messaddeq, S.J. Ribeiro, *Mater. Lett.*, 2009, **63(9-10)**, 797-799.
29. L. Hong, Y.L. Wang, S.R. Jia, Y. Huang, C. Gao, Y.Z. Wan, *Mater. Lett.*, 2006, **60**, 1710-1713.
30. Y. Hagiwara, A. Putra, A. Kakugo, H. Furukawa, J.P. Gong, *Cellulose*, 2010, **17(1)**, 93-101.
31. T. Maneerung, S. Tokura, R. Rujiravanit, *Carbohyd. Polym.*, 2008, **72(1)**, 43-51.
32. M. Chen, H. Kang, Y. Gong, J. Guo, H. Zhang, R. Liu, *ACS Appl. Mater. Inter.*, 2015,

7(39), 21717-21726.

33. G. Li, A.G. Nandgaonkar, Q. Wang, J. Zhang, W.E. Krause, Q. Wei, L.A. Lucia, *J. Membrane. Sci.*, 2017, **525**, 89-98.
34. C. Katepetch, R. Rujiravanit, *Carbohyd. Polym.*, 2011, **86(1)**, 162-170.
35. W. Hu, S. Chen, Z. Yang, L. Liu, H. Wang, *J. Phys. Chem. B*, 2011, **115(26)**, 8453-8457
36. S. Kirdponpattara, A. Khamkeaw, N. Sanchavanakit, P. Pavasant, M. Phisalaphong, *Carbohyd. Polym.*, 2015, **132**, 146-155.
37. H. Yano, J. Sugiyama, A.N. Nakagaito, M. Nogi, T. Matsuura, M. Hikita, K. Handa, *Adv. Mater.*, 2005, **17(2)**, 153-155.
38. K. Sano, Y. Ishida, T. Aida, *Angew. Chem. Int. Edit.*, 2018, **57(10)**, 2532-2543.
39. A. Weber, J. M. Murray, *Physiol. Rev.*, 1973, **53**, 612-673.
40. E. Proksch, J. M. Brandner, J.-M. Jensen, *Exp. Dermatol.*, 2008, **17**, 1063-1072.
41. A. J. S. Fox, A. Bedi, S. A. Rodeo, *Sports Health*, 2009, **1**, 461-468.
42. M. Hofinger, G. Bertholdt, D. Weuster‐Botz, *Biotechnol. Bioeng.*, 2011, **108(9)**, 2237-2240.
43. A. Nakagaito, H. Kondo, H. Takagi, *J. Reinf. Plast. Compos.*, 2013, **32(20)**, 1547-1552.
44. V. Palaninathan, N. Chauhan, A.C. Poulose, S. Raveendran, T. Mizuki, T. Hasumura, *et, al*, *Mater. Express.*, 2014, **4(5)**, 415-421.

Chapter 1.

Rapid uniaxial actuation of layered bacterial cellulose/poly (*N*-isopropylacrylamide) composite hydrogel with high mechanical strength

1.1 Introduction

As described in general introduction, anisotropic swelling and deswelling of hydrogels are essential for their utilizations in biomedical fields. Many biological systems have well-defined anisotropic structure, which is beneficial to carry out particular functions, including mass transport, surface lubrication, and force generation[1]. As a representative example, in a muscle sarcomere, actin and myosin show an anisotropic arrangement, which contributes the smooth motion of muscle fibers and muscle contraction in one direction while keeping other the direction constant[2-4]. Unfortunately, synthesized hydrogels are usually isotropic due to their preparation methods, which leads to homogeneous movement in response to external stimuli. Thus their applications in this field are greatly limited.

Poly(*N*-isopropylacrylamide) (PNIPAAm) is one of the most investigated polymers for preparing hydrogel actuators. It undergoes reversible lower critical solution temperature (LCST) phase transition from a swollen hydrated state to a shrunken dehydrated state. LCST of PNIPAAm hydrogel is close to body temperature and relatively insensitive to other environmental conditions such as pH and light, which makes PNIPAAm suitable for biomedical application[5]. Previously, anisotropic movement of PNIPAAm-based hydrogels has been successfully achieved[6-10]. However,

the volume changes of the PNIPAAm hydrogels are known to proceed very slowly[11,12], which indicates unsatisfactory responsive rate. Fast actuation in response to temperature change is often important for smart hydrogels. Furthermore, like other hydrogels, common PNIPAAm hydrogels possess poor mechanical properties.

Bacterial cellulose (BC) pellicle is a promising candidate as polymer matrix to enhance PNIPAAm hydrogels. With good biodegradability and biocompatibility, BC pellicle becomes an ideal choice in biomedical and biotechnological fields. The excellent mechanical property of BC hydrogel makes it act as ideal reinforcing element in polymer matrix. Moreover, BC pellicle with layered structures can be prepared by static culture of certain bacteria[13]. This kind of anisotropic structure brings about mechanical anisotropy[14]. In spite of these outstanding features, pristine BC hydrogel lacks certain functions and properties (i.e., stimuli-responsive property), which limits its applications in various fields. Therefore, synthesis of BC composites has been conducted to address these limitations. Many researchers focus on the preparation of BC-based functional composites with other polymers or inorganic materials to enlarge the potential applications of BC[15,16]. However, during the preparation process of BC-based composite, the unique structure of BC may be changed or broken due to the invading materials, resulting in the decrease of physical strength. Modifications of BC nanofibers have been performed with glutaraldehyde, divinyl sulfone and epichlorohydrin whereas the toxicity of the cross-linkers remains a big problem. In a previous study in our lab, comparatively low toxic methylene diphenyl diisocyanate (MDI) was utilized to modify BC nanofibers, which successfully protected the layered structure of BC hydrogel[17] (shown in Figure 1-1). Therefore, MDI-modified BC hydrogel with anisotropic structure is very promising to prepare composite hydrogels

with various anisotropic properties.

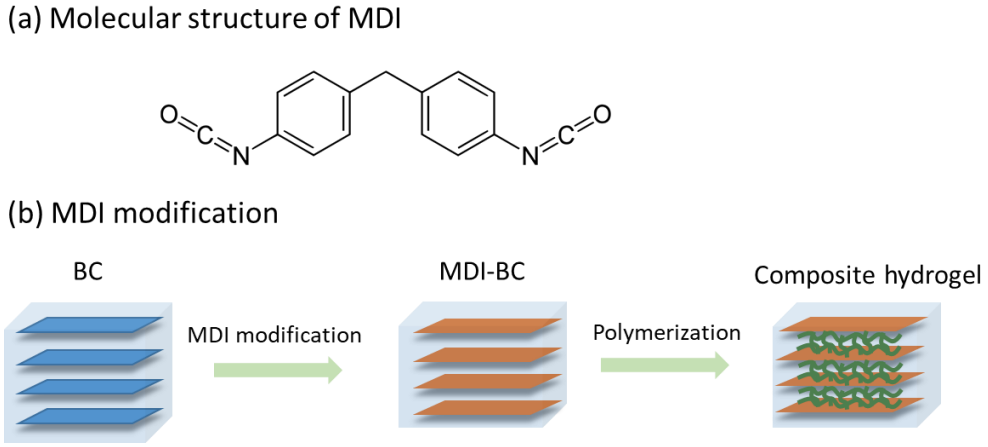

Figure 1-1. (a) Molecular structure of MDI and (b) schematic illustration of complex formation of MDI-modified BC-based composite with layered structure.

In this chapter, it was focused on the preparation of BC/PNIPAAm composite hydrogel by *in situ* polymerization method. Cellulose chains of BC were modified by MDI prior to the hydrogel formation with the purpose of protecting the unique layered structure of BC. The influence of the molar ratio of MDI/glucose unit of BC on the properties of the resulting hydrogel was investigated. With a certain MDI/glucose molar ratio, MDI-BC/PNIPAAm composite hydrogel with desired anisotropic structure, mechanical properties and responsive rate to temperature could be obtained. The anisotropic thermo-sensitivity of the present composite hydrogel was confirmed, indicating a possible application as artificial muscles with excellent recyclability.

1.2 Experimental

Materials

NIPAAm, ammonium persulfate (APS), MDI were purchased from Tokyo Chemical Industry Co., Ltd., Japan. *N,N′*-Methylenebisacrylamide (MBAAm) and *N,N,N′,N′*-tetramethyl-ethanediamine (TEMED) were obtained from Wako Pure Chemical Industries, Ltd., Japan. Triethylamine (TEA) and acetone were purchased from Nacalai Tesque, Inc., Japan. BC pellicles used in this experiment was prepared according to previous study in our lab[17].

Preparation of MDI-modified BC hydrogel

Medium of BC hydrogel was first exchanged with dehydrated acetone by immersing the BC hydrogel disc (1.5 g) into an excess of dehydrated acetone for 8 h under gentle shaking. Solvent replacement was repeated at least 3 times. A certain amount of MDI was then added to the acetone solution (20 mL) in the presence of the BC organogel, followed by the addition of TEA (76 μL). The molar ratio between MDI and the glucose unit of BC was set as 0.2:1, 1:1, and 2:1. The mixture was shaken at 25 ℃ for 3 h before it was kept at 50 ℃ for 48 h to form the MDI-modified BC organogel. The MDI-BC hydrogel was obtained by washing with acetone and deionized water.

Synthesis of MDI-modified BC/PNIPAAm composite hydrogel

NIPAAm monomer (1.0 g) and MBAAm (0.010 g) were first dissolved in deionized water (7.4 mL) to make the monomer solution. The MDI-BC disc (~1.6 g) was then immersed in the above solution for 12 h. APS (0.010 g) and TEMED (6.0 μL) were then added to start the polymerization. The whole weight of all the reagents and solvent was 10 g. After 12 h, the formed BC/PNIPAAm hydrogel was washed by

deionized water. The MDI-modified BC/PNIPAAm composite hydrogels were coded as COM1, COM2 and COM3 according to the molar ratio between MDI and the glucose unit of BC from 0.2:1 to 2:1. The BC/PNIPAAm hydrogel without the MDI modification, as a control, was coded as COM0.

Characterization

Fourier transform infrared spectroscopic analysis (FT-IR) was performed in an attenuated total reflectance (ATR) mode by a Nicolet iS5 Spectrometer (Thermo Fisher Scientific Inc., USA). SEM images were obtained on a HITACHI S-3500 instrument (Hitachi Co., Japan). The samples were lyophilized before the SEM observation. A compressive test was performed by a universal testing machine (EZ Graph, SHIMADZU, Japan). The samples (c.a. 20 mm in diameter and 10 mm in height) were fixed between two plates with compressive speed of 60 mm/min to obtain a typical stress-strain curve. The lower critical solution temperature (LCST) of the hydrogel samples was determined by a differential scanning calorimeter (EXSTAR 6000 DSC, Hitachi High-Tech Science Co., Japan). The thermal analysis was performed from 20 ℃ to 60 ℃ at the heating rate of 5 ℃/min under nitrogen. The onset point of the endothermal peak was used to determine the LCST[18,19].

Thermo-sensitive property measurement

For the equilibrium swelling ratio (ESR) measurement, the hydrogel samples were swollen in distilled water over a temperature range from 20 to 55 ℃, covering the LCST range of PNIPAAm hydrogel. The gravimetric method was employed; the samples were immersed in distilled water at predetermined temperature for 24 h to reach swelling equilibrium, and they were taken out and weighed after removing the excess water. ESR was calculated as follows:

$$swelling\ ratio = (W_s - W_d)/W_d \quad (1\text{-}1)$$

where W_s and W_d are the weight of the swollen and dried hydrogels, respectively.

The deswelling behaviors of the hydrogel were studied at 50 ℃ (above LCST) gravimetrically. At regular time intervals, the samples were taken out and weighed after removing the excess water. Water retention is defined as follows:

$$water\ retention = [(W_t - W_d)/(W_e - W_d)] \times 100 \quad (1\text{-}2)$$

Where W_t is the weight of the hydrogel at a determined time at 50 ℃, W_e is the weight of the hydrogel at equilibrated swelling at 20 ℃, and other symbols are the same as defined above.

For the anisotropic thermo-sensitive property, the samples were immersed in water at 50 ℃. l/l_0 and w/w_0 were shrinking (or deswelling) ratios parallel to the layer structure of BC/PNIPAAm hydrogel, and t/t_0 was that perpendicular, where l_0, w_0, t_0 were the length, width and thickness of the gel samples at equilibrium state in 20 ℃ solution and l, w, t were those at determined time at 50 ℃ in water solution .The length, width and thickness of the hydrogel samples were measured by a caliper.

1.3 Results and Discussion

Morphology and composition of the obtained composite hydrogels

The dry weights of the samples during each step were measured and summarized in Table 1-1. It can be calculated that the molar ratios between MDI and the glucose unit of BC (after reaction) were 0.19:1, 0.98:1 and 1.77:1 for COM1, COM2 and COM3, respectively. Similarly, the weight ratio of PNIPAAm in the final dried products could be calculated as 89%, 86%, 73% and 60% for COM0, COM1, COM2

and COM3, respectively, indicating successfully prepared PNIPAAm hydrogels in the presence of a hydrophobically modified BC matrix.

Table 1-1 Dry weights of all the samples after each step[a]

	COM0	COM1	COM2	COM3
MDI-BC (mg)	-	22	43	64
MDI : glucose unit of BC (mol : mol)	-	0.19:1	0.98:1	1.77:1
BC/PNIPAAm or MDI-BC/PNIPAAm (mg)	160	161	161	161
Weight ratio of PNIPAAm (wt%)	89%	86%	73%	60%

[a] Dry weights of BC in all the samples were 17 mg.

MDI-modified BC/PNIPAAm composite hydrogels were also studied by FT-IR spectra (Figure 1-2). Despite the difference in the MDI/glucose unit molar ratios, all the samples showed very similar FT-IR spectra. A sharp absorption peak at 3300 cm^{-1} is assigned to hydroxyl groups of BC chain. The samples had peaks at 1640 and 1540 cm^{-1} which are referred to the amide I and amide II of PNIPAAm, respectively. Notice that there was no obvious difference between the spectrum of COM0 hydrogel and those of

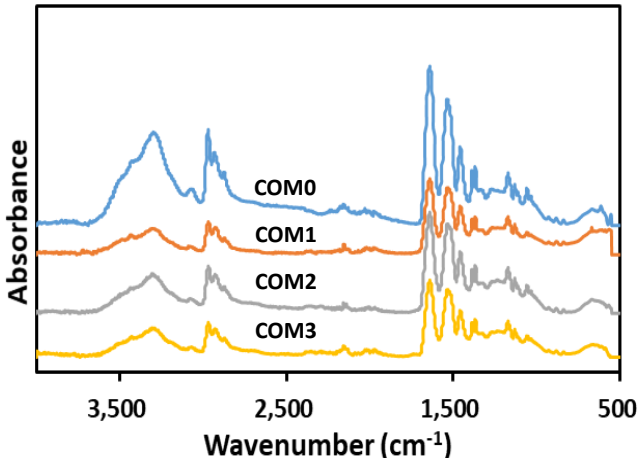

Figure 1-2. FT-IR spectra of BC/PNIPAAm hydrogel with different MDI ratios.

COM1, COM2, COM3. This is probably due to the reason that the IR spectrum of the urethane group derived from MDI is similar to that of PNIPAAm with the amide group.

According to the SEM images of pure BC hydrogel (Figures 1-3a and b), the 3D network structure of BC was confirmed in the horizontal image while it showed an

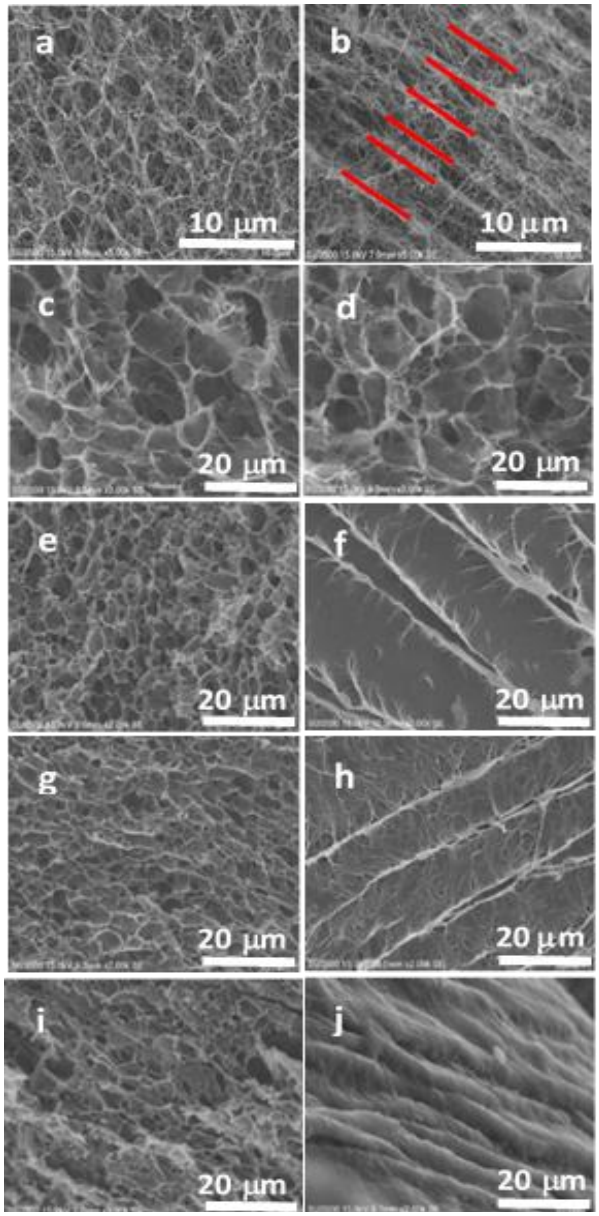

Figure 1-3. SEM images of pure BC (a and b), COM0 (c and d), COM1 (e and f), COM2 (g and h), COM3 (i and j). Horizontal and vertical images are on the left and right columns, respectively. Red bars indicate the layered structure of BC.

excellent layered structure in the vertical direction, indicating the anisotropic structure of BC hydrogel. However, the BC/PNIPAAm hydrogel (COM0) might partially (or completely) lose this layered structure (Figure 1-3d) due to the formation of PNIPAAm hydrogel, resulting in porous morphology. When cellulose chains of BC were cross-linked by MDI before the polymerization of PNIPAAm, the layered structure in the vertical direction could preserve to some extent (Figures 1-3f, h and j) while the horizontal images displayed the 3D network structure. It's assumed that cellulose chains within the same layer of BC network were cross-linked by MDI rather than those between different layers. The more the MDI ratio, the better the layered structure inside the hydrogel remained. Thus the average thickness of the layers decreased with increasing the MDI ratio and the average thickness of COM3 was close to that of pure BC hydrogel. The SEM observation indicates that the anisotropic composite hydrogels were successfully prepared. This unique structure was believed to endow special properties to the hydrogels, which would be mentioned below.

Mechanical properties of the composite hydrogels

Figure 1-4 shows the stress-strain curves of the composite hydrogels including pure BC hydrogel in the vertical direction (perpendicular to the layered structure), whereas data obtained from these tests can also be found in Table 1-2. The data prove that the introduction of BC and MDI-modified BC matrix would greatly improve the mechanical property of PNIPAAm hydrogel. The maximum compressive strength of COM0 was 532 kPa whereas that of PNIPAAm hydrogel was 20 kPa. With the increase of the MDI/glucose unit ratio, the compressive strength increased gradually. COM3 had the largest compressive strength of 838 kPa, which was about 40 times of that of the PNIPAAm hydrogel. This significant improvement of mechanical strength is believed to

be beneficial to various applications. The SEM images show that the composite hydrogel with the higher MDI/glucose unit ratio has the smaller layer thickness, making the sample more rigid. As a result, the MDI-modified BC/PNIPAAm hydrogel with the higher MDI/glucose unit ratio would have better mechanical strength.

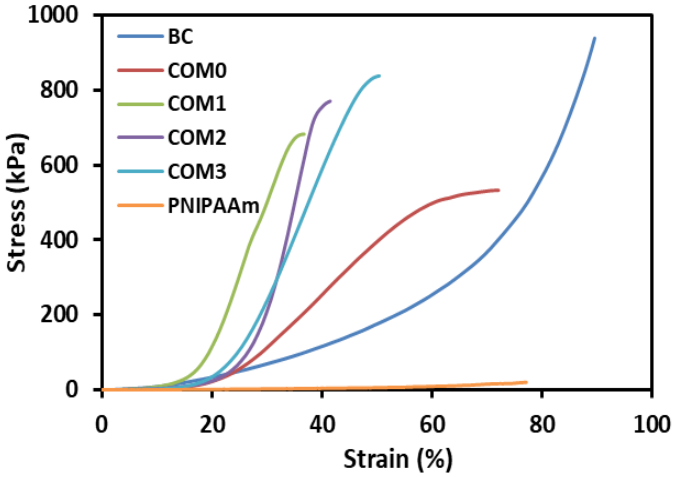

Figure 1-4. Stress-strain curves of BC/PNIPAAm composite hydrogels with different MDI ratio, BC and PNIPAAm hydrogels under compression.

Table 1-2 Mechanical properties of BC, PNIPAAm and BC/PNIPAAm composite hydrogels with different MDI ratio.

Sample	Compressive strength (kPa)	Strain at break (%)
BC	938	89
COM0	532	72
COM1	682	36
COM2	770	41
COM3	838	50
PNIPAAm	20	77

Thermo-sensitive property

The lower critical solution temperature (LCST) of the series of the hydrogel samples were examined by DSC (Figure 1-5a). The onset temperature of endotherm was referred as LCST. Obviously, all the samples showed almost the same LCST at about 32 ℃, which matched well with the LCST of PNIPAAm hydrogel. From these data, the BC or MDI-modified BC nanofibers were found to have little impact on LCST of PNIPAAm, indicating that the networks of BC (or MDI-BC) and PNIPAAm are chemically identical and no reaction occurred between them. It is well known that LCST is the point where the hydrophobic interaction of the isopropyl group of PNIPAAm outweighs the hydrophilic nature of the amide group in the pendant group, forcing water out of the hydrogel. The subsequent research and applications are mainly based on this LCST of the composite hydrogel.

The temperature dependence of equilibrium swelling ratio (ESR) is shown in Figure 1-5b. The swelling data here showed that all the samples had similar classical thermo-responsive profile. The ESR of all the hydrogels decreased dramatically toward their LCST and had the sharpest decrease around 32 ℃ where the phase separation

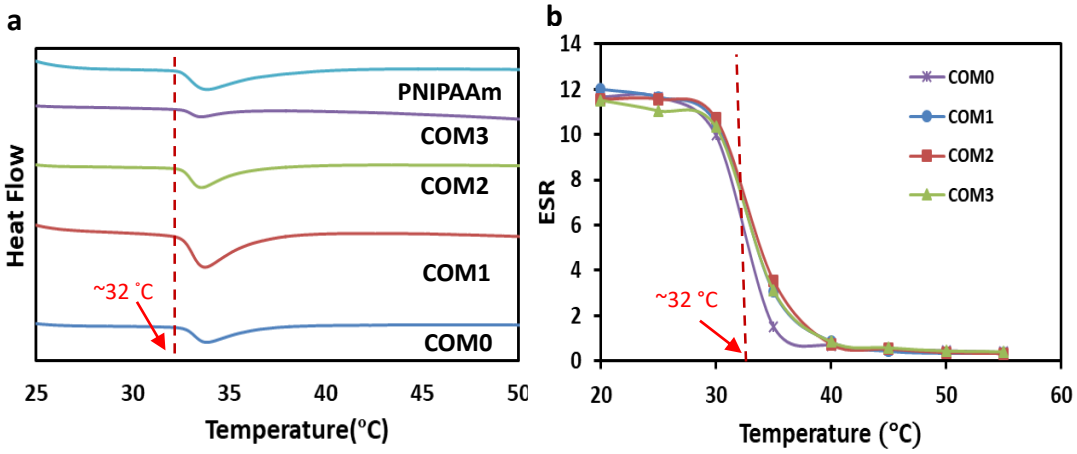

Figure 1-5. (a) DSC traces of swollen hydrogel samples; (b) ESR of the composite hydrogels in the temperature range from 20 ℃ to 55 ℃

occurred. Above the LCST, the hydrogel samples showed almost the same level of ESR regardless of the MDI ratio difference. The LCST from the ESR observation is in good agreement with the thermal data of the DSC study.

Figure 1-6 exhibits the deswelling behaviors of the composite hydrogels in water at 50 ℃ (above LCST). After 20 h, all the five hydrogels including PNIPAAm had a similar water retention of around 3~4% (data not shown in Figure 1-6). However, the composite hydrogels showed the relatively faster response to this temperature in the initial 60 min, i.e., COM3 lost about 40% water in the first 10 min whereas pure PNIPAAm hydrogel only lost less than 15% water in the same time period. About 76% water was freed from COM3 in 30 min whereas PNIPAAm showed only 43% water release in the same time frame. The order of water lose rate within 30 min was COM3>COM2>COM1>COM0>PNIPAAm. The composition between BC and PNIPAAm networks as well as the MDI modification significantly improved the responsive rate of the hydrogel. Generally, PNIPAAm-based hydrogels present slow responding property to temperature. For example, Okano *et al.* reported that only 15% volume shrinkage was observed for a PNIPAAm-based hydrogel disk for 60 min on heating from 10 to 40 ℃[11]. Up to now, three main kinds of strategies have been developed to improve the response rate of PNIPAAm-based hydrogels as follows: (1) diminishing the dimension of hydrogels, (2) generating porous structures of hydrogels, and (3) chemically modifying polymeric networks of hydrogels[12]. In our case, the size of PNIPAAm gel in the BC/PNIPAAm composite was reduced mainly due to the layered BC matrix, leading to the rapid response to temperature change. On the other hand, the PNIPAAm-based hydrogels usually form dense hydrophobic layers on outmost surface – so-called skin layers above LCST[20], which results in slow volume

change. BC chains with high hydrophilicity in the BC/PNIPAAm composite hydrogels may inhibit the formation of the skin layers, which would induce the increase in the response rate of the composite hydrogel.

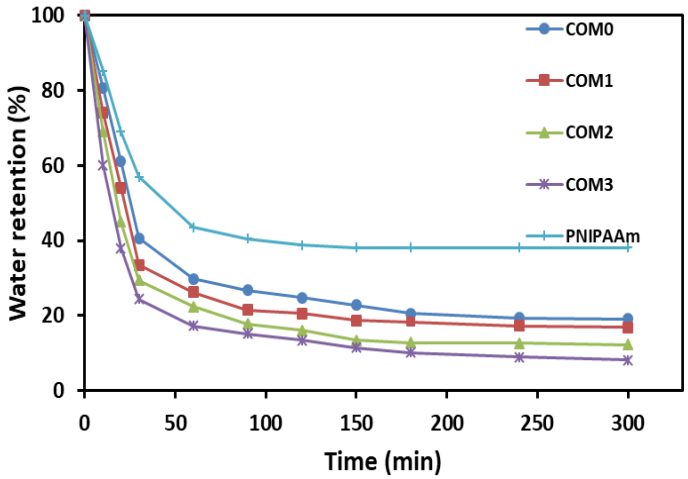

Figure 1-6. Deswelling behaviors of the composite hydrogel samples at 50 ℃

Commonly, PNIPAAm-based hydrogels have a homogeneous structure, resulting in an isotropic thermo-sensitive property. On the other hand, the anisotropic structure of the present MDI-modified BC/PNIPAAm hydrogels as shown in the SEM images influences the thermo-sensitiveness. As shown in Figure 1-7a, COM3 clearly exhibited the uniaxial deswelling behavior in response to temperature change. The thickness of the hydrogel decreased gradually whereas the length and width remained almost unchanged. The photos of uniaxial deswelling of COM3 above LCST are shown in Figure 1-7b. The equilibrium deswelling of the hydrogels with different MDI ratios above the LCST is concluded in Figure 1-7c. In the direction perpendicular to the layered structure (vertical), COM0, COM1, COM2 and COM3 shared a similar thickness deswelling ratio (t/t_0) of about 20%. However, the deswelling ratio parallel to

the layered structure (horizontal) gave the different result: l/l_0 and w/w_0 of COM0 were less than 80% whereas those of COM1, COM2 and COM3 were more than 95%. In the

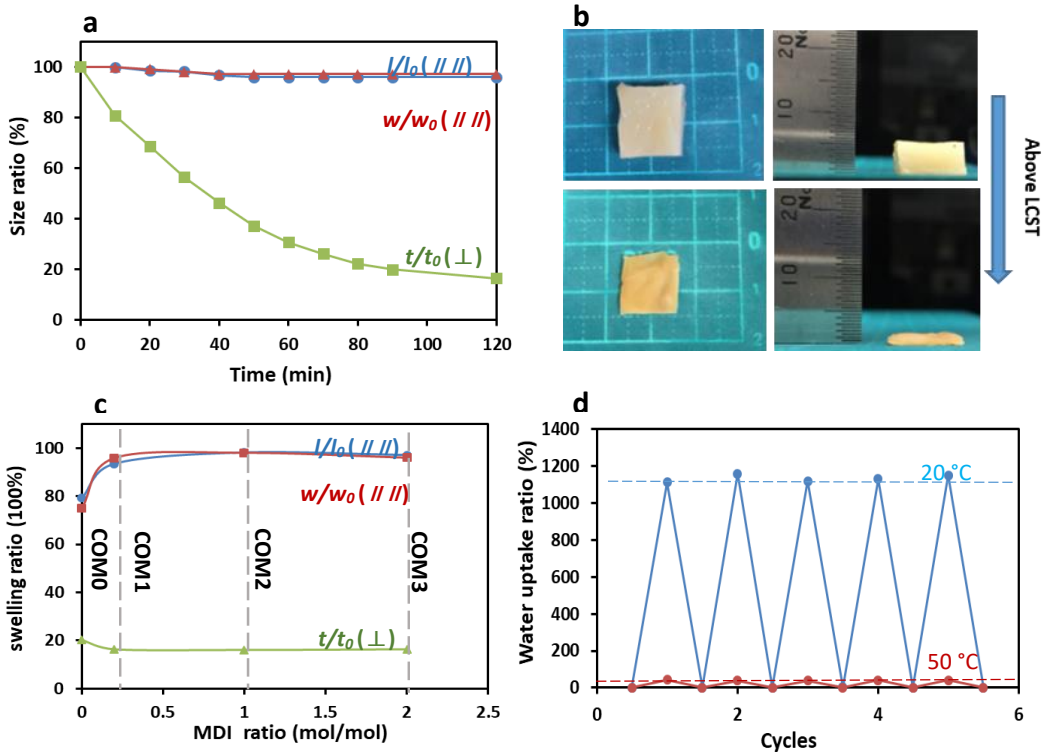

Figure 1-7. (a) Length (l), width (w) and thickness (t) change of COM3 above LCST with time; (b) photos of uniaxial deswelling of COM3 above LCST for 120 min. Left and right images indicate top and side views, respectively; (c) anisotropic deswelling of the hydrogels with different MDI ratios above the LCST; (d) repeatable swelling behavior of COM3 gel below or above LCST.

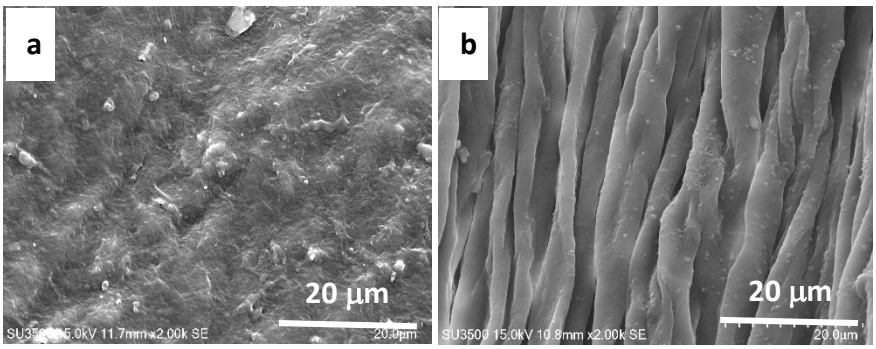

Figure 1-8. SEM images of dried COM3: (a) horizontal and (b) vertical images are on the left and right columns, respectively.

present composite hydrogel, the PNIPAAm network could swell freely only in the direction perpendicular to the BC layers whereas in other two directions (parallel to the layers), the swelling was almost completely restricted by the rigid BC layers, resulting in the uniaxial deswelling-swelling. Once deswelling above LCST, the BC/PNIPAAm gel could swell back to its original hydrogel state below LCST. This process was reversible and easily controlled by temperature change. Figure 1-7d shows the repeatable swelling behavior of dried COM3 below or above LCST. It hardly absorbed any water at 50 ℃ because PNIPAAm showed hydrophobicity above LCST. However, at 20 ℃ the dried COM3 swelled well and absorbed a large amount of water (> 1000% of the dried gel weight) to recover back to its original hydrogel state. Moreover, the water uptake ability of COM3 almost remained unchanged below or above LCST after many cycles, indicating the desired recyclability of the present composite hydrogel. The SEM images of the dried composite gel (COM3) were shown in Figure 1-8. Visibly, the BC fibrils arranged randomly in the horizontal direction whereas in the vertical direction the sample showed the excellent layered structure. Therefore, the BC fibrils in the dried composite gel are still arranged in an anisotropic manner.

1.4 Conclusion

In this study, a novel MDI-modified BC/PNIPAAm composite hydrogel was developed by in situ polymerization and the changes in morphology, mechanical properties, response rate to temperature, and thermo-sensitive properties were elucidated. Only the MDI-modified BC/PNIPAAm composite hydrogel exhibited an anisotropic layered structure in which the average layer thickness of the hydrogel decreased with the increase of the MDI/glucose molar ratio. It was clearly observed that

the composition between BC and PNIPAAm networks as well as MDI modification contributed to the reinforcement of PNIPAAm gel and the present hydrogel exhibited 40 times higher compressive strength than neat PNIPAAm gel. Besides, the composite hydrogel showed improved response rate to temperature which depended on the MDI/glucose molar ratio. This controllable response rate is significant for future practical applications. Furthermore, the anisotropic thermo-sensitivity of the composite hydrogel was revealed due to the reason that the gel only swelled and deswelled perpendicular to the layers uniaxially. The unique temperature-responsive property as well as enhanced physical strength and adjustable response rate makes the MDI-modified BC/PNIPAAm composite hydrogel a promising choice in biomedical fields such as artificial muscles.

1.5 References

1. K. Sano, Y. Ishida, and T. Aida, *Angew. Chem., Int. Ed.*, 2018, **57(10)**, 2532-2543.
2. M. Haque, G. Kamita, T. Kurokawa, K. Tsujii and J. P. Gong，*Adv. Mater.*, 2010, **22(45),** 5110-5114.
3. J. A. Spudich, R. S. Rock, *Nat. Cell. Biol.*, 2002, **4**, 8.
4. M. A. Geeves, *Nature*, 2002, **415**, 129.
5. J. F. Lutz, Ö. Akdemir, A. Hoth, *J. Am. Chem. Soc.*, 2006, **128(40)**, 13046-13047.
6. T. Asoh, E. Kawamura, A. Kikuchi, *RSC Adv.*, 2013, **3**, 7947-7952.
7. Y. S. Kim, M. J. Liu, Y. Ishida, Y. Ebina, M. Osada, T. Sasaki, T. Hikima, M. Takata and T. Aida, *Nat. Mater.*, 2015, **14**, 1002-1007.
8. A. S. Gladman, E. A. Matsumoto, R. G. Nuzzo, L. Mahadevan, J. A. Lewis, *Nat. Mater.*, 2016, **15**, 413-418.
9. N. Miyamoto, M. Shintate, S. Ikeda, Y. Hoshida, Y. Yamauchi, R. Motokawa, M. Annaka, *Chem. Commun.*, 2013, **49**, 1082-1084.
10. R. M. Erb, J. S. Sander, R. Grisch and A. R. Studart, *Nat. Commun.*, 2013, **4**, 1712.
11. R. Yoshida, K. Uchida, Y. Kaneko, K. Sakai, A. Kikuchi, Y. Sakurai, T. Okano, *Nature*, 1995, **374**, 240-242.
12. L. W. Xia, X. J. Ju, J. J. Liu, R. Xie, L. Y. Chu, *J. Colloid. Interf. Sci*., 2010, **349**, 106-113.
13. D. Ciechańska, *Fibres. Text. East. Eur.*, 2004, **12(4)**, 69-72.
14. A. Nakayama, A. Kakugo, J. P. Gong, Y. Osada, M. Takai, T. Erata, S. Kawano, *Adv. Funct. Mater.*, 2004, **14(11)**, 1124-1128.
15. J. Kim, Z. Cai, H. S. Lee, G. S. Choi, D. H. Lee and C. Jo, *J. Polym. Res.*, 2011, **18(4)**, 739-744.

16. Z. Shi, S. Zang, F. Jiang, L. Huang, D. Lu, Y. Ma and G. Yang, *RSC Adv.*, 2012, **2(3)**, 1040-1046.
17. H. Shim, X. Xiang, M. Karina, L. Indrarti, R. Yudianti and H. Uyama, *Chem. Lett.*, 2015, **45(3)**, 253-255.
18. X.Z. Zhang, Y.Y. Yang, T.S. Chung and K.X. Ma, *Langmuir*, 2001, **17(20)**, 6094-6099.
19. X.Z. Zhang, C.C. Chu, *Polymer*, 2005, **46(23)**, 9664-9673.
20. A. S. Hoffman, A. Afrassiabi, L. C. Dong, *J. Control. Release.*, 1986, **4**, 213-222.

Chapter 2.

Facile fabrication of flexible bacterial cellulose/silica composite aerogel for oil/water separation

2.1 Introduction

With frequent oil spill accidents worldwide, exploration and development of efficient, large-scalable, and economic methods to clean oil spills is becoming urgent. Compared with the traditional in situ burning[1], bioremediation[2], and dispersants[3], hydrophobic three-dimensional porous materials with high specific surface areas which have strong ability to absorb oil or organic liquid from water phase is a facile approach for oil spills clean-up. Among these, hydrophobized silica aerogels (SAs) is a promising choice due to its nanoporous structure and excellent hydrophobicity. However, the inherent fragility and comparatively high cost have restricted the wide application of SAs[4]. Some efforts have been taken to endow flexibility to SAs using alkyltrialkoxysilane instead of the traditional tetraethoxysilane (TEOS) precursor[5-7]. Nevertheless, the preparation process of silica aerogels can not adapt to commercial scale production since supercritical drying and expensive reagents are often required.

Bacterial cellulose (BC) aerogel is a promising potential oil sorbent due to its ultralow density, high specific surface area and low cost. However, BC aerogel has to be tailed (or modified) in order to convert its inherent hydrophilicity to hydrophobicity to ensure that it exhibits excellent oil/water selectivity[8]. Moreover, once compressed, BC aerogel is not able to recover back to its original shape, indicating its weak elasticity and reusability. Some researchers try to solve these problems by the construction of an

interpenetrating network structure of a BC matrix and a silica skeleton (shown in Figure 2-1). Although the mechanical properties of BC/silica composite aerogels have been improved to some extent, the flexibility of the aerogels still need to be enhanced so that they can be utilized as reusable and recyclable oil sorbents[9,10]. Expensive or toxic reagents are used to prepare elastic BC/silica aerogel, which is not suitable for large-scalable and green industrial manufacturing[11,12].

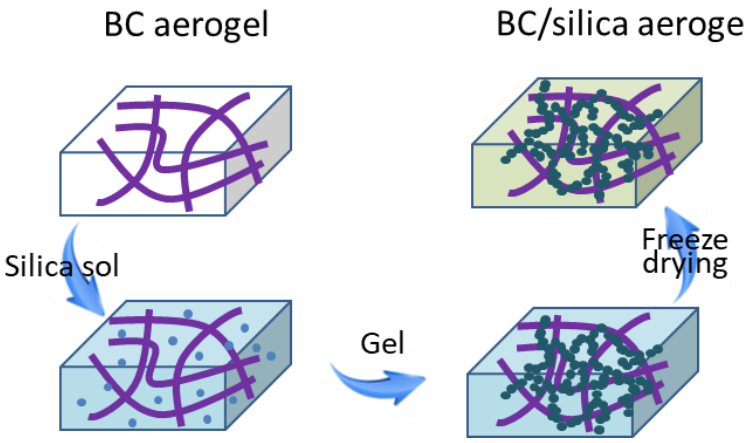

Figure 2-1. Schematic illustration of the formation mechanism of the BC/silica composite aerogel.

In this study, as a substitute of BC aerogel, methylene diphenyl diisocyanate (MDI)-modified BC aerogel was introduced to fabricate BC/silica composite aerogel *via* the sol-gel process followed by freeze-drying. The silica aerogel was prepared from methyltrimethoxysilane (MTMS) in the presence of BC matrix. The morphology, hydrophobicity, mechanical property and oil absorption ability of the composite were systematically investigated. This research aims to develop a facile and cost-effective method to prepare BC/silica composite aerogel with good oil/water separation ability, which is an ideal oil sorbent for oil spill clean-up and water purification.

2.2 Experimental

Materials

Methylene diphenyl diisocyanate (MDI) was purchased from Tokyo Chemical Industry Co., Ltd., Japan. Acetic acid and sodium hydroxide (NaOH) were obtained from Wako Pure Chemical Industries, Ltd., Japan. Triethylamine (TEA), acetone and methanol were purchased from Nacalai Tesque, Inc., Japan. Methyltrimethoxysilane (MTMS) was provided by Kanto Chemical Co., Inc., Japan. Acetone was completely dehydrated before use. BC matrix was purified from *Nata-de-coco* (unpurified BC pellicle).

Fabrication of MDI-modified BC aerogel

BC hydrogel was first exchanged with dehydrated acetone to get BC organogel, followed by the addition of MDI and triethylamine (TEA). The molar ratio between MDI and the glucose unit of BC was set as 2:1. This solution was stirred at 25 ℃ for 3 h before kept at 50 ℃ for 48 h to get MDI-BC organogel. After solvent exchange with acetone and deionized water, the desired MDI-BC aerogel was obtained after freeze-drying.

Preparation of MDI-modified BC/silica aerogel

First, methyltrimethoxysilane (MTMS) (1.44 mL), methanol (5 mL) and acetic acid (1 mol/L, 0.72 mL) were mixed, stirred for 1 h. After 24 h, MDI-BC aerogel was immersed into the above solution, followed by the addition of 0.72 mL 10 mol/L ammonia water. After stirred for 30 min, the MDI-BC gel was taken out and started gelation at room temperature for 24 h. After solvent exchange with methanol and water, the MDI modified BC/silica aerogel was prepared by freeze-drying (Scheme 2-1). As control, BC/silica aerogel without MDI modification was also prepared with the same

method.

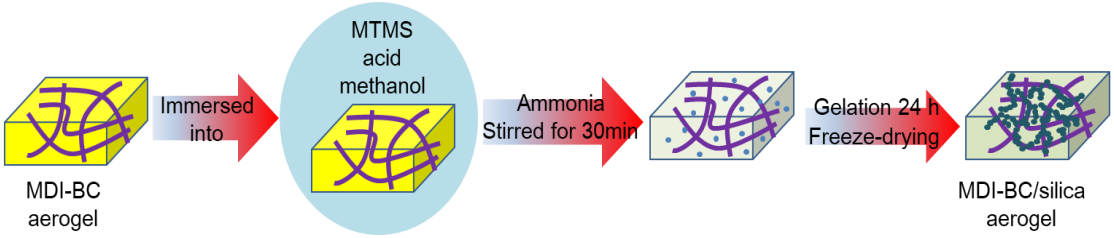

Scheme 2-1. Fabrication process of MDI-BC/silica composite aerogel

Characterization

Fourier transform infrared spectroscopic analysis (FT-IR) was performed in an attenuated total reflectance (ATR) mode by a Nicolet iS5 Spectrometer (Thermo Fisher Scientific Inc., USA). The microstructure of aerogel was recorded by scanning electron microscope (SEM, Hitachi Co., SU3500). Contact angles of the samples were measured with a Drop Master DM300 (Kyowa Interface Science). Water droplet with a volume of 1.0 μL was fixed onto the surface and the contact angle was determined at 2 s (scanning time) after the attachment of the droplet. Compressive test was performed by using a Haake Rheostress-6000 (Thermo Electron) with parallel plate geometry. The absorption abilities of the aerogels (Q) toward various oils and organic liquids were calculated by the equation:

$$Q = (W_s - W_d)/W_d \quad (2\text{-}1)$$

where W_d and W_s are the weight of the aerogels before and after complete absorption in a certain solvent.

2.3 Results and Discussion

Morphology and hydrophobicity

The functional groups of the obtained aerogels were estimated from the FT-IR spectra (Figure 2-2). Due to the reaction between cellulose chains of BC and MDI, the intensity of the -OH peak in MDI-BC was weaker than that of neat BC aerogel. The peaks observed around 1250 cm^{-1} and 1050 cm^{-1} were assigned to Si-C bending and Si-O stretching band, respectively, which indicated successful preparation of BC/silica and MDI-BC/silica composite aerogels. It can also be noted that only MDI-BC and MDI-BC/silica aerogels exhibited peaks at around 1700 cm^{-1} which corresponded to C=O stretching, resulting from the MDI modification.

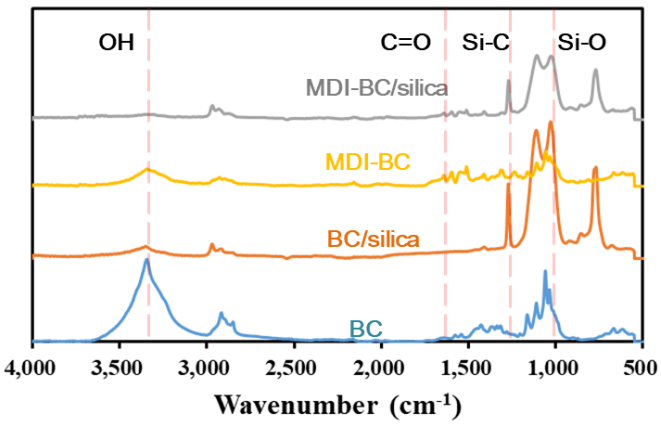

Figure 2-2. FT-IR spectra of BC, MDI-BC, BC/silica and MDI-BC/silica aerogels

The SEM images of the obtained aerogels are shown in Figure 2-3. BC aerogel clearly showed the typical three-dimensional (3D) porous and fibrous network structure

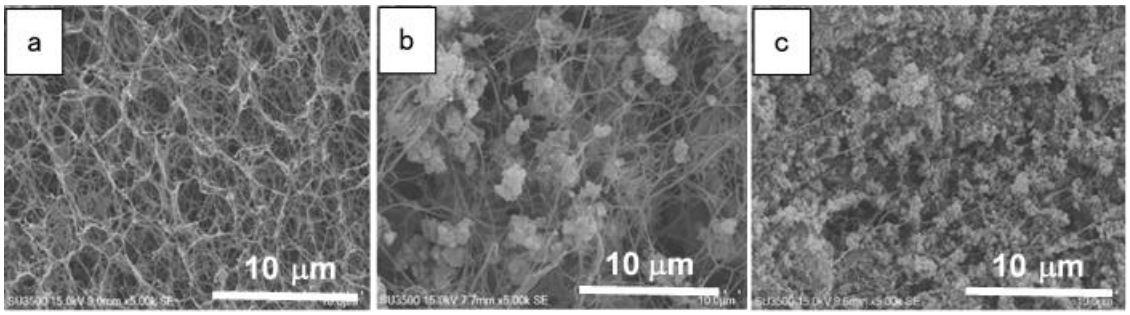

Figure 2-3. SEM images of (a) BC aerogel; (b) BC/silica aerogel; (c) MDI-BC/silica aerogel.

(Figure 2-3a). Due to the obvious difference between hydrophilic BC network and hydrophobic silica skeleton, silica particles aggregated prior to being distributed uniformly in the BC matrix (Figure 2-3b). As a consequence, large silica particles formed at the junctions of cellulose fibers, leading to a comparatively inhomogeneous structure. On the other hand, the MDI modification improved the hydrophobicity of BC nanofibers. Then smaller silica particles covered on cellulose fiber in case of MDI-BC/silica aerogel (Figure 2-3c). The uniform structure of the present composite aerogel are beneficial for the enhancement of hydrophobicity as well as mechanical properties.

The contact angles of the samples were exhibited in Figure 2-4. The MDI-BC/silica aerogel possessed an improved contact angle (134) than the BC/silica aerogel (117), indicating that hydrophobic MDI-BC/silica aerogel is more beneficial for oil absorption from water. The MDI-BC aerogel exhibited a contact angle of around

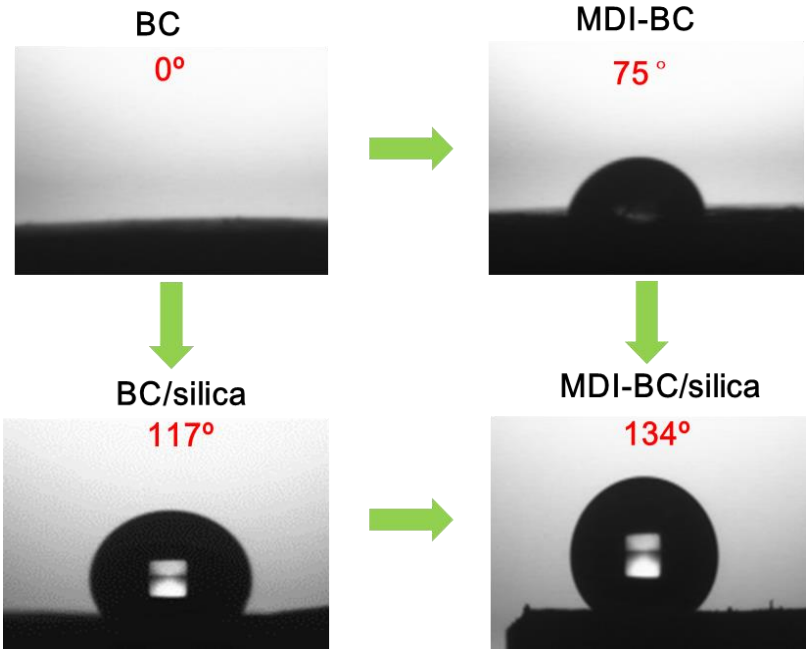

Figure 2-4. Contact angles of BC, MDI-BC, BC/silica, and MDI-BC/silica aerogels.

75 °, which was much higher than that of neat BC aerogel (~0 °). The reaction between cellulose chains of BC and MDI should be the reason for the improvement of hydrophobicity. A conclusion could also be made that the improved hydrophobicity between MDI-BC/silica and BC/silica seemed to come from the MDI modification.

Mechanical properties of the composite aerogels

Cyclic compressive tests were performed to measure the mechanical properties of the aerogels (Figure 2-5). BC aerogel, as expected, showed low compressive stress (ca. 24 kPa, Figure 2-5a) and once compressed, it could not recover to its initial shape after unloading the stress (Figure 2-5b). Compared with BC aerogel, the mechanical strength of BC/silica aerogel was significantly enhanced. The compressive stress in cycle 1 was 565 kPa (Figure 2-5a), which was about 24 times of that of BC aerogel. However, the stress-strain curves in cycle 2 and cycle 3 were not smooth, which may be attributed to the cracks formed in the aerogel during the compression process (Figure 2-5c). The mechanical property was further improved in MDI-BC/silica aerogel and it showed a compressive stress of 669 kPa in cycle 1 (Figure 2-5a). In comparison to the BC/silica aerogel, the MDI-BC/silica aerogel showed improved mechanical strength mainly due to the reason that the MDI modification improved the hydrophobicity of the BC matrix, leading to a more homogeneous structure between MDI-BC network and the silica skeleton (Figure 2-3). Compared with the first cycle, the second and third cycles showed a slightly decrease of compressive stress (Figure 2-5d), which was caused by the rearrangement of the MDI-modified BC networks in the presence of the silica skeleton. In all cycles, the MDI-BC/silica aerogel recovered to its original state as shown in inset images in Figure 2-5d. These superior mechanical properties and

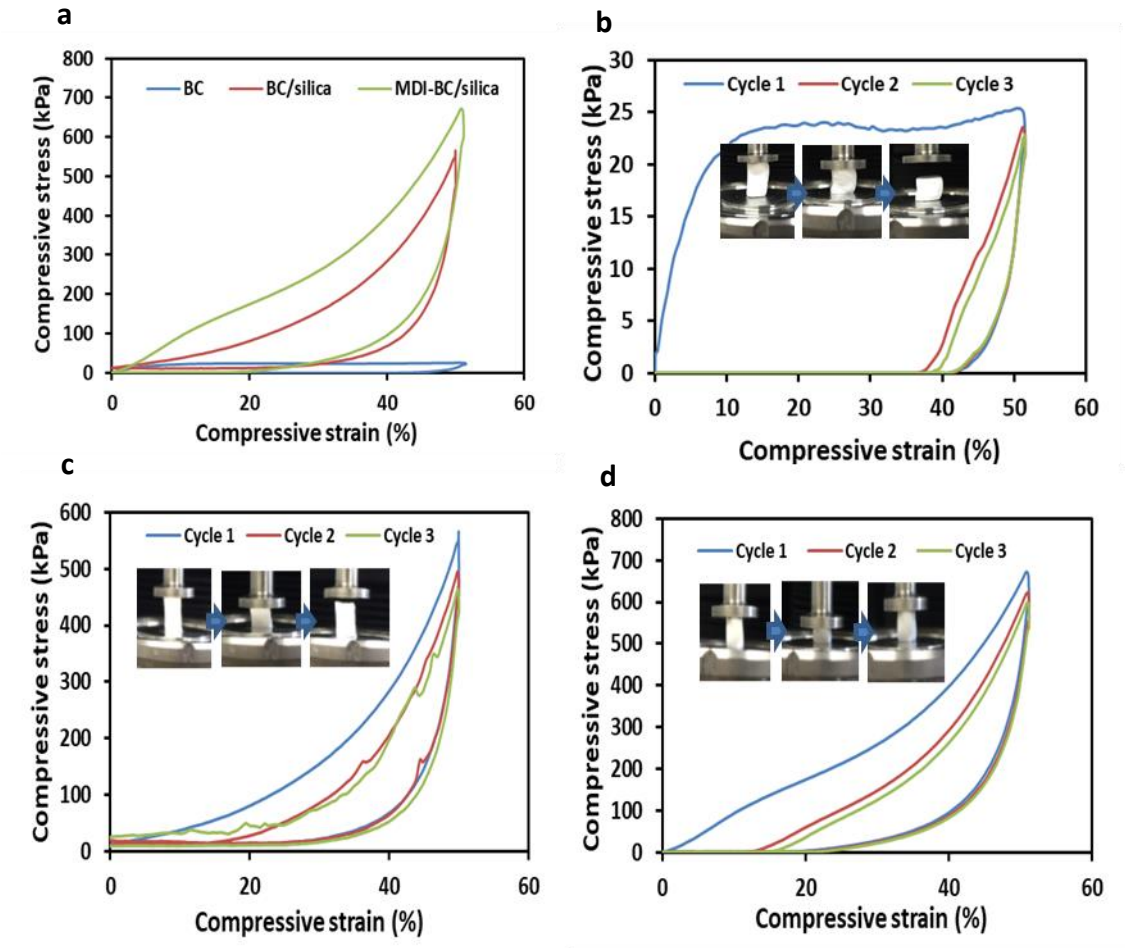

Figure 2-5. (a) Compressive stress-strain curves of BC, BC/silica and MDI-BC/silica aerogels in Cycle 1; Cyclic compressive stress-strain curves of (b) BC aerogel, (c) BC/silica aerogel and (d) MDI-BC/silica aerogel at a maximum strain of 50% (inset: photos of aerogel during the test).

effective shape recovery capability are of crucial importance for the application of oil collection from water and recovery by squeezing.

Oil absorption capacity

Because of the porous structure, high flexibility, and hydrophobicity, the obtained MDI-BC/silica aerogel is a promising material for oil/water separation. As shown in Figure 2-6, the sample was placed in a mixture of water/plant oil (dyed with oil red). After saturated absorption, the sample could be easily removed from the

mixture due to its low density and excellent floatability. By simply squeezing the samples, the absorbed plant oil was collected. Due to the homogeneous structure between BC matrix and silica skeleton, no silica particles got out of the composite aerogel during the process. The oil was completely separated from the water phase by repeating the absorption/squeezing process several times. The obtained oil with little water could further be utilized in other applications. Moreover, the aerogel could be easily reused by washing with acetone or ethanol followed with freeze-drying. The volume and shape change of the composite aerogel during this process was almost negligible, indicating the satisfactory reusability which was necessary for ideal oil sorbent.

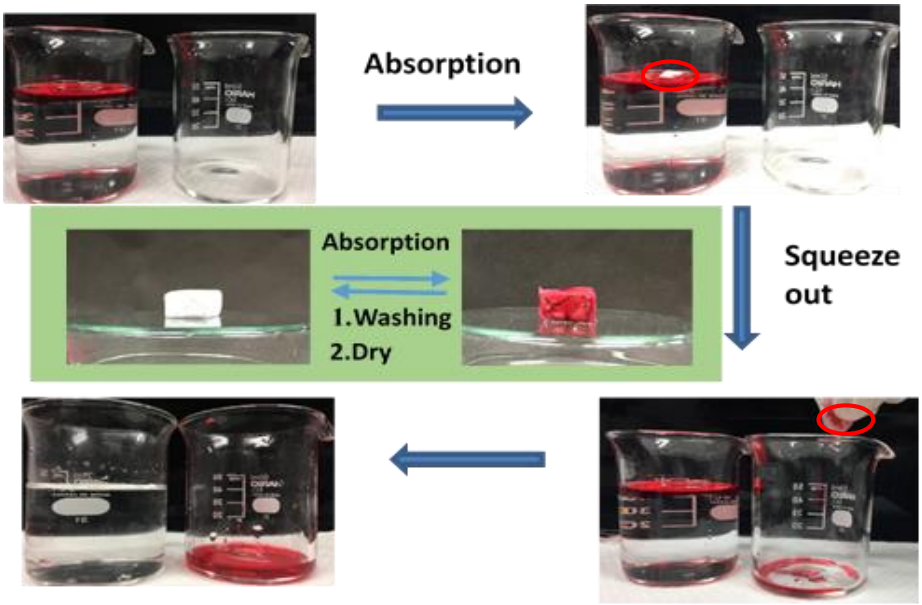

Figure 2-6. The absorption of plant oil (dyed with oil red) and recovery of the MDI-BC/silica aerogel.

Figure 2-7 presented the absorption capability of the composite aerogels toward several common organic liquids. The MDI-BC/silica composite aerogel could absorb up to 5-15 times (Figure 2-7a) of its own dry weight and this absorption ability

was proportional to the densities of the absorbed solvent. The polarity of the organic solvents only affected the initial absorption rate by the aerogel. However, this absorption process finished in a very short period of time to reach the saturated absorption, making the differences of polarity almost negligible. For all of the solvents used in this experiment, MDI-BC/silica aerogel exhibited better absorption capability than BC/silica aerogel. Especially, when toluene was used as a model oil, it was found that the oil absorption capability of BC/silica aerogel was only about 83% of that of MDI-BC/silica aerogel. Better silica skeleton and improved hydrophobicity of the MDI-modified composite aerogel might be reasons for the oil absorption ability

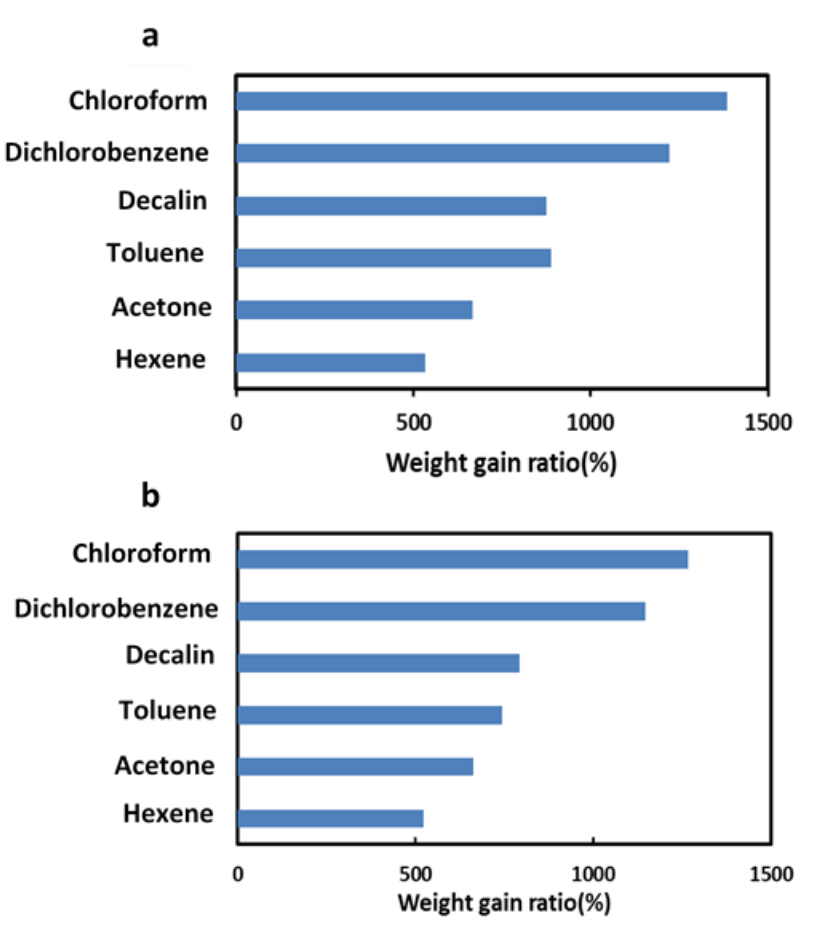

Figure 2-7. Absorption capacities of (a) MDI-BC/silica aerogel; (b) BC/silica aerogel toward different organic liquids.

difference existing in BC/silica and MID-BC/silica aerogels. Therefore, the MDI-BC/silica aerogel with better oil absorption capability is more suitable as oil sorbent.

The recyclability of the composite aerogel was investigated by repeating the oil absorption-washing-drying process, the results of which were summarized in Figure 2-8a. It could be observed that even after 5 cycles the absorption amount of MDI-BC/silica aerogel was still 93% of the initial value. Moreover, the morphology of the present composite aerogel remained almost unchanged after 5 cycles with uniform silica skeleton covering the cellulose fibers (Figure 2-8b). The relatively constant value

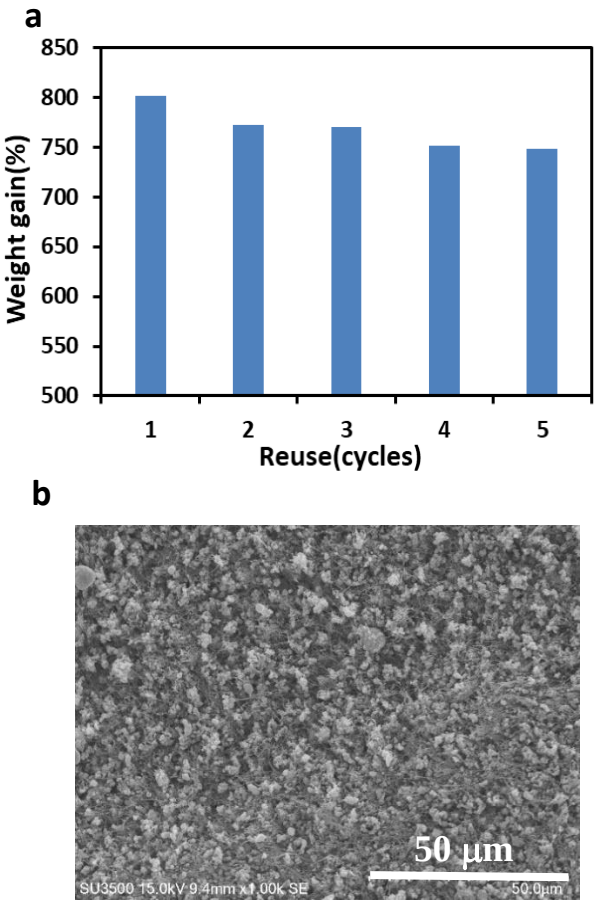

Figure 2-8. (a) Absorption recyclability of the MDI-BC/silica aerogel toward dichlorobenzene; (b) SEM image of MDI-BC/silica aerogel after 5 cycles of oil absorption.

of absorption capability and stable structure confirmed the recyclability and reusability of the MDI-BC/silica aerogel.

2.4 Conclusion

In this study, cellulose chains of BC was firstly modified by MDI via a feasible liquid-phase reaction and the obtained MDI-BC aerogel was further used to prepare the MDI-modified BC/silica aerogel through a simple sol-gel process followed by freeze-drying. The MDI-modification significantly improved the contact angle of BC aerogel, leading to a comparatively uniform structure between BC network and hydrophobic silica skeleton in the MDI-BC/silica composite aerogel. As a result of the synergic effects of the MDI-BC matrix and silica, the obtained aerogel showed excellent flexibility and robustness which overcame the fragility of pure silica aerogel and low elasticity of pure BC aerogel. The MDI-BC/silica aerogel possessed excellent hydrophobicity with a contact angle of 134° and excellent porous structure, resulting in the satisfactory absorptivity for a wide variety of organic solvents and oils. Along with the desiring flexibility and recyclability, this MDI-BC/silica composite aerogel became an ideal oil sorbent for oil spill clean-up and water purification.

On the other hand, it is better to decrease the amount of MTMS used in the preparation process and further improve the oil absorption capacity of the composite aerogel so that the present composite aerogel can adapt to practical industrial production.

2.5 References

1. Q. Lin, I. A. Mendelssohn, K. Carney, S. M. Miles, N. P. Bryner, and W. D. Walton, *Environ. Sci. Technol.*, 2005, **39(6)**, 1855-1860.
2. J. R. Bragg, R. C. Prince, E. J. Harner and R. M. Atlas, *Nature*, 1994, **368(6470)**, 413-418.
3. E. B. Kujawinski, M. C. Kido Soule, D. L. Valentine, A. K. Boysen, K. Longnecker and M. C. Redmond, *Environ. Sci. Technol.*, 2011, **45**, 1298-1306.
4. J. L. Gurav, A. V. Rao, D. Y. Nadargi, H. H. Park, *J. Mater. Sci.*, 2010, **45**, 503-510.
5. A. V. Rao, S. D. Bhagat, H. Hirashima and G. M. Pajonk, *J. Colloid. Interf. Sci.*, 2006, **300(1)**, 279-285.
6. D. Y. Nadargi, S. S. Latthe, H. Hirashima and A. V. Rao, *Micropor. Mesopor. Mat.*, 2009, **117**, 617-626.
7. K. Kanamori, M. Aizawa, K. Nakanishi and T. Hanada, *Adv. Mater.*, 2007, **19(12)**, 1589-1593.
8. H. Sai, R. Fu, L. Xing, J. Xiang, Z. Li, F. Li and T. Zhang, *ACS Appl. Mater. Inter.*, 2015, **7(13)**, 7373-7381.
9. H. Sai, L. Xing, J. Xiang, L. Cui, J. Jiao, C. Zhao, Z. Li, F. Li and T. Zhang, *RSC adv.*, 2014, **4(57)**, 30453-30461.
10. H. Sai, L. Xing, J. Xiang, L. Cui, J. Jiao, C. Zhao, Z. Li and F. Li, *J. Mater. Chem. A*, 2013, **1(27)**, 7963-7970.
11. J. He, H. Zhao, X. Li, D. Su, F. Zhang, H. Ji and R. Liu, *J. Hazard. Mater.*, 2018, **346**, 199-207.
12. H. Sai, R. Fu, J. Xiang, Y. Guan and F. Zhang, *Compos. Sci. Technol.*, 2018, **155**, 72-80.

Chapter 3.

Facile preparation of a novel transparent composite film based on bacterial cellulose and atactic polypropylene

3.1 Introduction

The last few decades have witnessed the rapid development of new transparent films for food packaging, electronic and optoelectronic devices[1,2]. Bacterial cellulose (BC) nanofibers show very promising characteristics as reinforcement material for optically transparent plastics[3]. Known as "*nata-de-coco*", BC is able to be produced in large scales and low cost by bacteria such as *Acetobacter xylinum*. Compared with widely used plant-derived cellulose, BC-derived film has several advantages such as high crystallinity, high purity and porosity. Especially, the high crystallinity of BC film results in excellent mechanical strength of high Young's Modulus and tensile strength. Along with its high specific surface area and excellent moldability, BC film exhibits its fascinating potential as reinforcing element in polymer matrix[4,5].

Many kinds of polymers have been explored for the fabrication of transparent composite films with BC. Such BC-based composite films maintain the remarkable properties of BC film while preserving the ease of bending of pure polymers. Very recently, polydiethyleneglycol–bisallyl carbonate, poly(lactic acid), hemiaminal, and poly(vinyl alcohol) were investigated[6-9]. The main drawback of BC-based composite films is their hygroscopicity resulting from the hydroxyl groups of cellulose chains, leading to moisture absorption and spoiling the thermal stability and high strength of BC. Therefore, hydrophobic polymers are usually applied to convert the inherent

hydrophilicity of BC nanofibers into hydrophobicity in order to avoid the hygroscopicity of the composite film. Besides, the polymers should be cheap and nontoxic so that the composite films can be adapted to commercial scale production.

Atactic polypropylene (*at*-PP) is a promising candidate to form composite film with BC. It is an inevitable noncrystalline byproduct with very low molecular weight obtained during polymerizing propylene into isotactic polypropylene (*it*-PP)[10]. Due to its poor heat resistance and mechanical properties, its usage and application fields are limited. Taking the large amount of *at*-PP remained in industrial production of *it*-PP into consideration, it is an emergent task to find new application fields to make effective use of *at*-PP.

To our best knowledge, there have been no reports on the composites of BC and *at*-PP. In this study, considering the benefits and drawbacks of BC film and *at*-PP, the author attempted to prepare a BC/*at*-PP composite film by a facile "sandwich" hot-press method (Scheme 3-1). The transparency, morphology, hydrophobicity, mechanical properties and thermal stability of the composite film were carefully investigated and compared with neat BC and *at*-PP films.

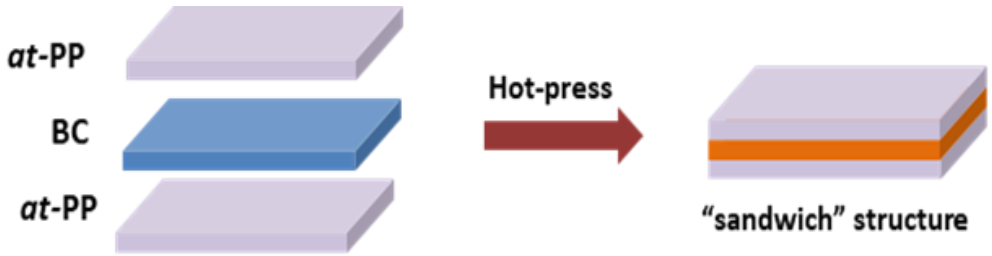

Scheme 3-1. Schematic illustration of complex formation of sandwich-like BC/*at*-PP composite film.

3.2 Experimental

Materials

Atactic polypropylene (*at*-PP, amorphous PP) and isotactic polypropylene pellets (*it*-PP, M_w ~250,000) were purchased from Sigma-Aldrich (USA). Methanol was obtained from Nacalai Tesque, Inc., Japan. BC pellicle was kindly supplied by Fujicco Co., Ltd., Japan and purified according to our previous work. In brief, the initial BC hydrogel sheets were washed with deionized water for 3 days and immersed in boiling 2% aqueous NaOH solution. Finally, it was rinsed with deionized water until pH became neutral. No further chemical modification for *at*-PP or BC was carried out.

Fabrication of BC and at-PP films

BC pellicles were cut into strips using a razor with the following dimensions, ~60×15×10 mm and then exchanged with methanol thoroughly so that the subsequent hot-press could be carried out in a lower temperature, avoiding the carbonization of cellulose. The BC samples were then hot-pressed at 2 MPa and 80 ℃ for 4 min followed by cooling down for 3 min to obtain dried BC sheets (~25 μm). *at*-PP pellets were melted at 170 ℃ for 2 min in a thin steel mold and then compressed at 12 MPa for 10 min. After cooled to room temperature for 3 min, thin *at*-PP film (~60 μm) was prepared and cut into strips with the same size as the dried BC sheets.

Fabrication of BC/at-PP composite film

For the preparation of BC/*at*-PP composite film, one dried BC sheet was sandwiched between two *at*-PP films and heated at 170 ℃ for 2 min. After compressed at 12 MPa for 10 min, BC/*at*-PP composite film was obtained after a 3 min cooling process. Although a temperature of 170 ℃ was applied during the hot-press procedure, the resulting composite film was transparent, colorless and no carbonization of cellulose

occurred.

Fabrication of it-PP and BC/it-PP films

As control, neat *it*-PP and BC/*it*-PP films were also prepared. Similar to the preparation of *at*-PP film, *it*-PP pellets were melted at 230 ℃ for 2 min in a thin steel mold and then compressed at 12 MPa for 10 min. After cooled to room temperature for 3 min, thin *it*-PP film was prepared and cut into strips with the same size as the dried BC sheets. For BC/*it*-PP composite film preparation, one dried BC sheet was sandwiched between two *it*-PP films and heated at 230 ℃ for 2 min. After compressed at 12 MPa for 10 min, BC/*it*-PP composite film was obtained after a 3 min cooling process. Due to the comparatively high hot-press temperature (230 ℃) required to melt *it*-PP pellets, the obtained composite film turned to yellow resulting from the pyrolysis of BC.

Characterization

The optical transmittance of the films were measured from 300 to 850 nm using a Hitachi U2810 UV-visible spectrophotometer. The microstructure of the films were observed by scanning electron microscope (SEM, Hitachi Co., SU3500). Fourier transform infrared spectroscopic analysis (FT-IR) was performed in an attenuated total reflectance (ATR) mode by a Nicolet iS5 Spectrometer (Thermo Fisher Scientific Inc., USA). Contact angles of the samples were measured with a Drop Master DM300 (Kyowa Interface Science). Water droplet with a volume of 1.0 μL was fixed onto the surface and the contact angle was determined at 2 s (scanning time) after the attachment of the droplet. Tensile test was carried out by using a universal testing machine (EZ Graph, SHIMADZU, Japan). Thermogravimetric analysis (TGA) was performed with an EXSTAR TG/DTA 7200 thermogravimetric analyzer (Hitachi High-Tech Science Co.,

Japan) from 40 to 550 ℃ at a heating rate of 10 ℃/min under a flowing nitrogen atmosphere.

3.3 Results and Discussion

Transparency of the films

The optical images of BC, *at*-PP and BC/*at*-PP films were shown in Figures 3-1a, b and c, respectively. The blue picture behind the BC film was almost invisible in Figure 3-1a whereas *at*-PP (Figure 3-1b) and BC/*at*-PP films (Figure 3-1c) exhibited

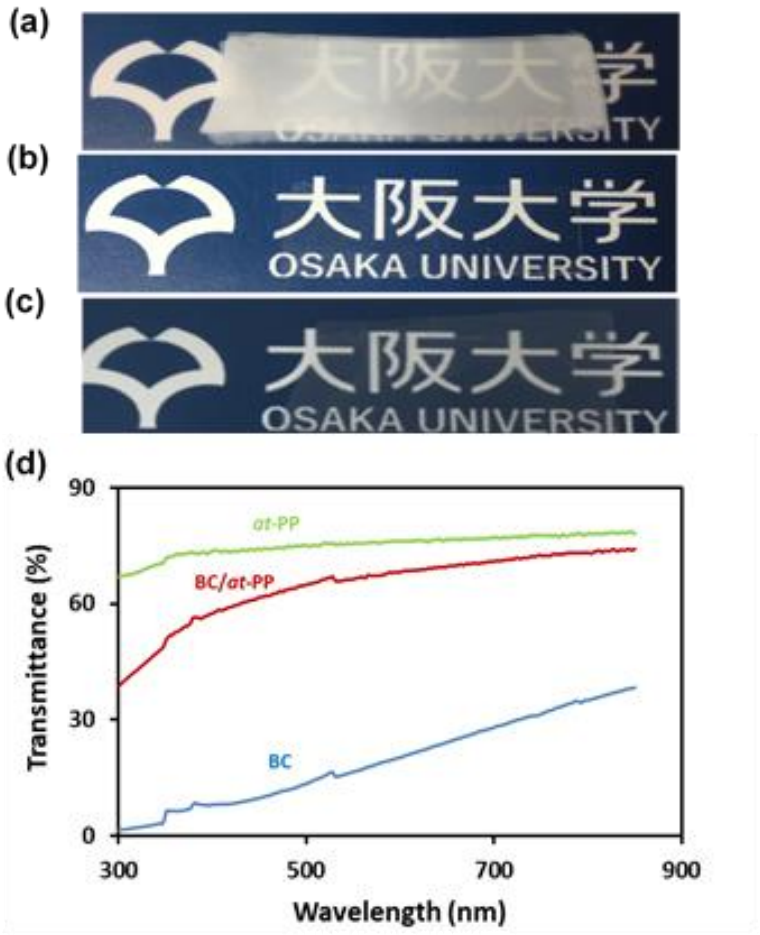

Figure 3-1. Images of (a) opaque BC film, (b) transparent *at*-PP film and (c) BC/*at*-PP composite film. (d) Transmittance of BC, *at*-PP, and BC/*at*-PP films in the UV-visible wavelength region.

transparent appearance. The transmittances of BC, *at*-PP and BC/*at*-PP films in the wavelength range between 300 and 850 nm were shown in Figure 3-1d. The pristine BC film, as expected, displayed very poor transparency with a transmittance value of 38% at 850 nm. Compared with the BC film, the BC/*at*-PP composite film showed a significant increase in transparency with a transmittance of 74% at the same wavelength, which was quite close to that of neat *at*-PP film. It is well-known that the contrast between the refractive index of the BC cellulose fibers (η>1.5) and air (η=1.0) causes light scattering, leading to the low transparency of BC film[11]. On the other hand, the high transparency of the BC/*at*-PP composite film was obtained due to the reason that the interface between cellulose fibers and air disappeared by *at*-PP filling. Meanwhile, the refractive index of *at*-PP (η=1.45) was quite close to that of BC fibers (η=1.54) [12]. Another reason responsible for the good transparency of the composite film was that the diameter of BC nanofiber was between 10 ~ 60 nm. When the size of the filler was less than one-tenth of the visible light wavelength, light scattering was suppressed (nanosize effect), leading to the good transparency. [3,13]

Morphology and hydrophobicity

The SEM images of BC, *at*-PP and BC/*at*-PP films in the cross section were shown in Figures 3-2a, b and c, respectively. Obviously, the BC/*at*-PP composite film showed a sandwich-like structure (Figure 3-2c), resulting from the preparation method. The three-layer structure of the composite film was also confirmed from the FT-IR spectra since BC/*at*-PP and *at*-PP films showed similar curves and peaks (Figure 3-3), while those of BC film were quite different. A composite layer of about 25 μm was sandwiched between two layers of *at*-PP resin. The morphology of BC, *at*-PP and BC/*at*-PP films in the horizontal direction was exhibited in Figure 3-4. The *at*-PP resin

filled the pores of the BC network during the hot-press process and formed the comparatively dense surface structure, which might account for the good transparency of the composite film mentioned above. Calculated from weight changes, the BC fiber weight ratio was 40% in the composite film.

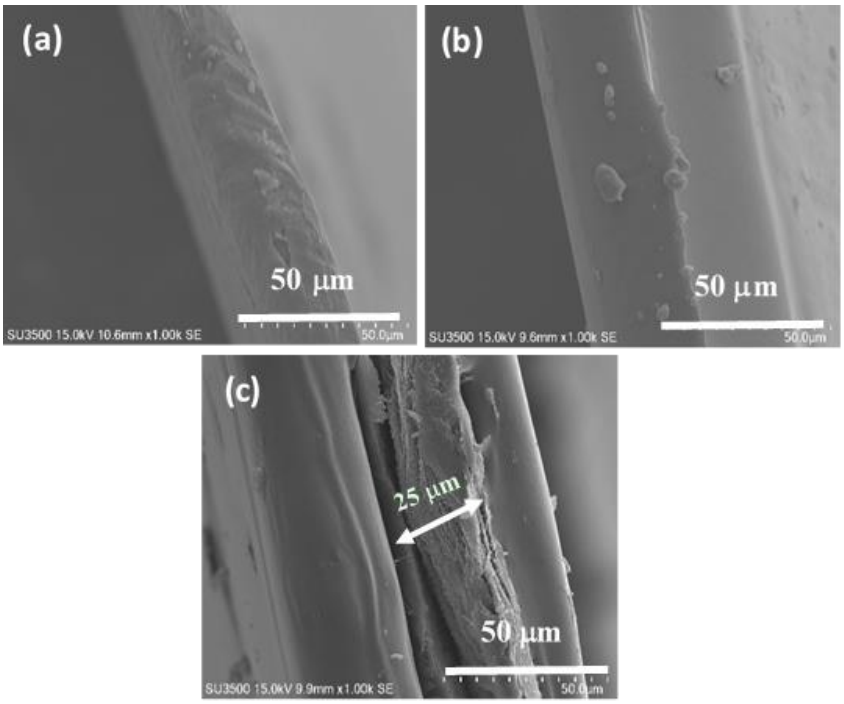

Figure 3-2. SEM images of (a) BC, (b) *at*-PP, and (c) BC/*at*-PP films in the cross section.

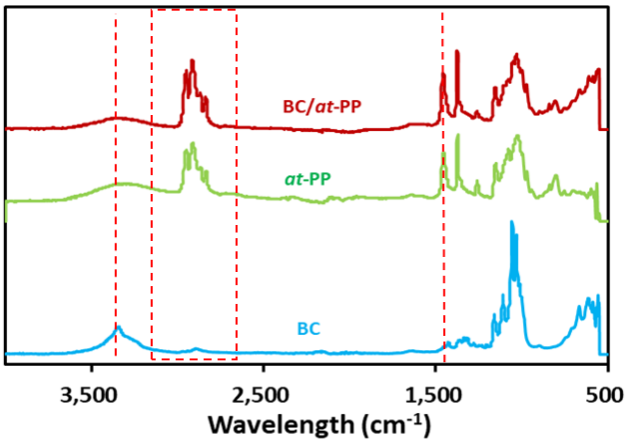

Figure 3-3. FT-IR spectra of BC, *at*-PP and BC/*at*-PP films.

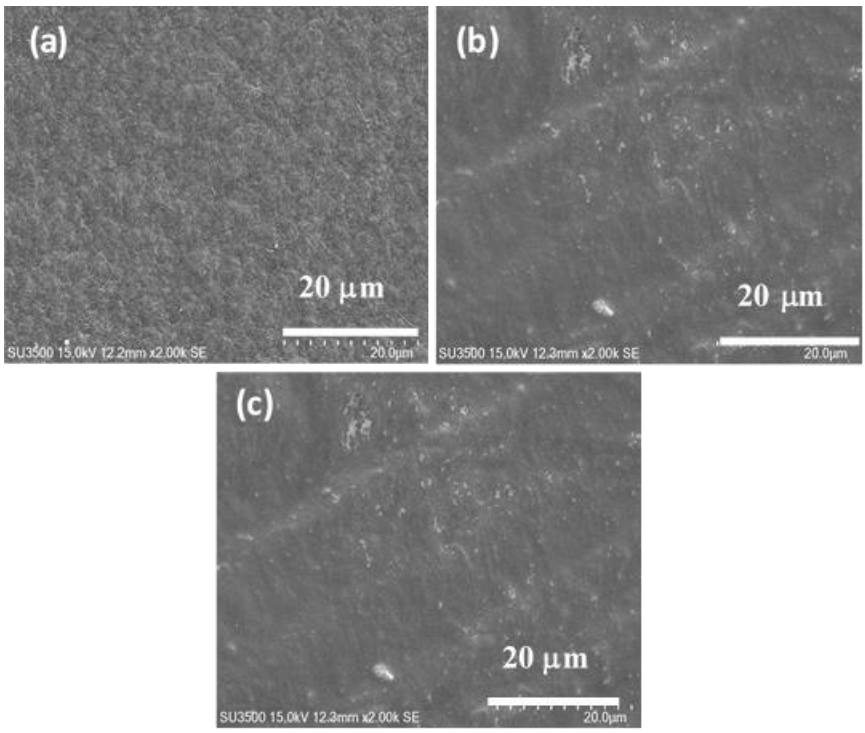

Figure 3-4. SEM images of (a) BC, (b) *at*-PP, and (c) BC/*at*-PP films in horizontal direction

It is well known that hydrophobic transparent films are desired in practical applications to avoid or decrease their hygroscopicity. Therefore, the contact angles of BC, *at*-PP and BC/*at*-PP films were measured and exhibited in Figure 3-5. The BC/*at*-PP composite film showed a contact angle of 104 °, which was much higher than that of neat BC film. Due to the sandwich structure, presenting of hydrophilic cellulose to outermost surface was inhibited by hydrophobic *at*-PP, which is beneficial to enlarge

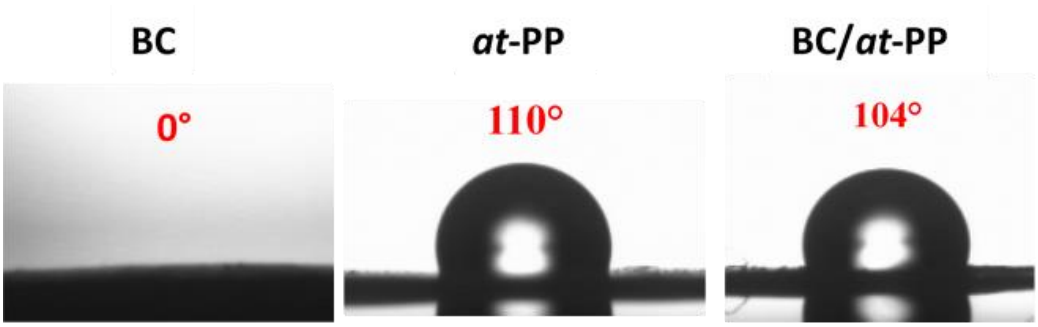

Figure 3-5. Contact angles of BC, *at*-PP, and BC/*at*-PP films on their surfaces.

the application fields of the composite film.

Mechanical properties of the composite films

Typical tensile stress-strain curves of BC, *at*-PP and BC/*at*-PP films were shown in Figure 3-6, whereas data obtained from these tests can also be found in Table 3-1. As a result of its amorphous nature, the tensile strength for *at*-PP film was found to

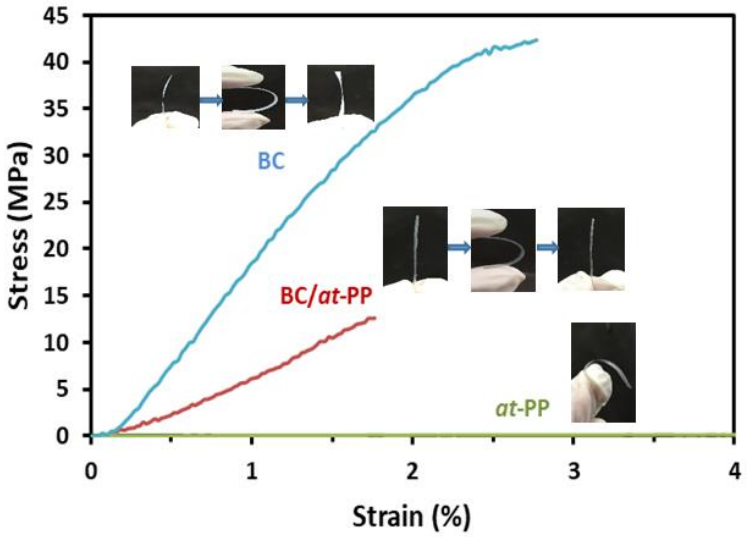

Figure 3-6. Tensile stress-strain curves for BC, *at*-PP and BC/*at*-PP films. (Inset images are the photos indicating the flexibility of the corresponding films)

Table 3-1. Mechanical properties of BC, *at*-PP[a] and BC/*at*-PP films.

	Tensile strength (MPa)	Strain at break (%)
BC	42	2.7
at-PP	0.28	15
BC/*at*-PP	13	1.8

[a] For convenience, only part of the stress-strain curve of *at*-PP was exhibited.

be extremely low (~0.28 MPa). On the other hand, the ultimate tensile strength of BC/*at*-PP film (~13 MPa) was about 46 times of that of *at*-PP film, indicating the good reinforcement effect of BC nanofibers to *at*-PP film. A tremendous increase of modulus was also obtained for the BC/*at*-PP composite film in comparison to *at*-PP film, which can be attributed to the excellent mechanical strength of the BC component. The decrease of the ultimate elongation of composite compared to pure BC film resulted from the extra entanglements and physical crosslinks between BC networks and *at*-PP chains, which confined the mobility of BC chains and hampered the change of network structure. Moreover, the present composite film maintained the excellent flexibility of neat BC film, whereas pure *at*-PP film was extremely soft and not flexible (Figure 3-6, inset images). Therefore, the weak mechanical properties of neat *at*-PP film was significantly enhanced by BC matrix whereas its good transparency remained almost unchanged, enlarging the potential application fields of *at*-PP.

Thermal properties

The thermal stability and degradation profiles of the films were assessed by thermogravimetry (Figure 3-7). The good thermal stability of BC film has already been proved by previous studies. The TGA tracing of the neat BC film exhibited a typical single weight-loss step due to the decomposition of cellulose chains, with a maximum decomposition rate at ~350 ℃. Due to the incorporation of *at*-PP, the BC/*at*-PP composite film showed two main degradation steps. The composite film started degradation at ~255 ℃ and reached a maximum weight loss rate at ~360 ℃ during the first step. Compared with pure BC film, the BC/*at*-PP composite film presented an increment by about 10 ℃ of both the initial and maximum degradation temperatures,

indicating the considerable thermal stability of the corresponding composite film.

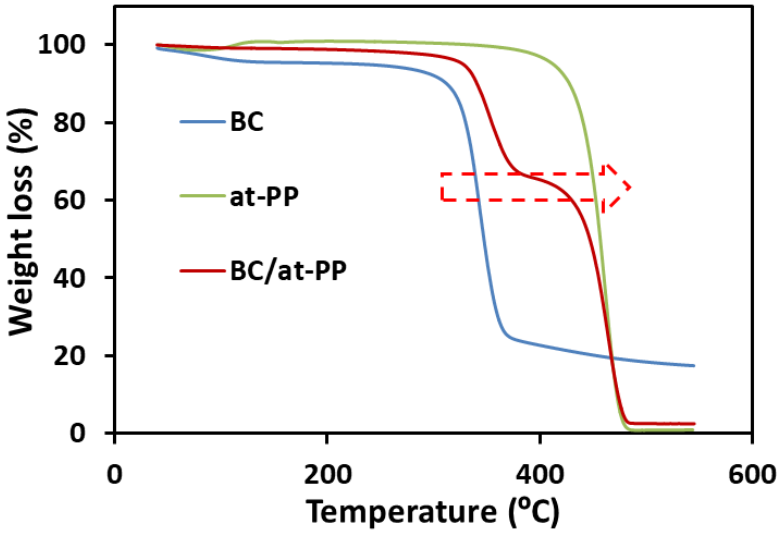

Figure 3-7. Thermogravimetric curves for BC, *at*-PP and BC/*at*-PP films.

Control experiment: properties of BC/it-PP composite film

As a contrast, BC/*it*-PP composite film was also prepared by the facile sandwich hot-press method and its most important properties were characterized.

The optical images of BC, *it*-PP and BC/*it*-PP films were shown in Figures 3-8a, b and c, respectively. Neat *it*-PP film exhibited good transparent appearance (Figure 3-8b) whereas the BC/*it*-PP composite film was translucent with yellow color (Figure 3-8c), which was due to the pyrolysis and carbonization of cellulose during the heating process. The transmittances of BC, *it*-PP and BC/*it*-PP films in the wavelength range between 300 and 850 nm were shown in Figure 3-8d. The *it*-PP film displayed good transparency with a transmittance value of 71% at 850 nm while that of BC/*it*-PP was only 51%. Such composite film with low transparency could not be used in practical applications.

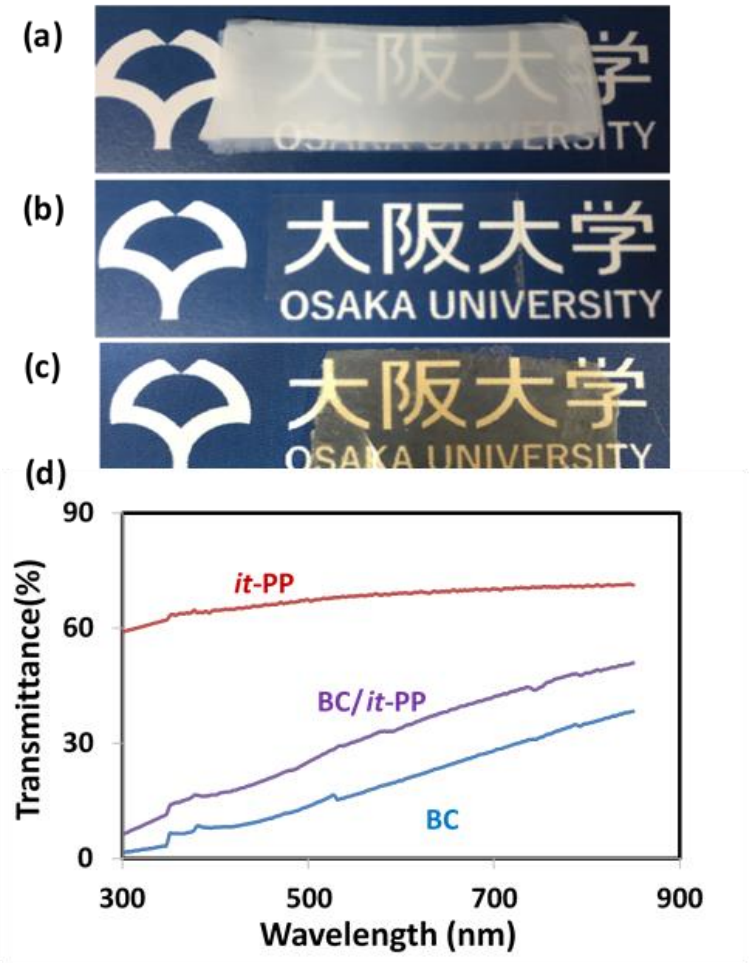

Figure 3-8. Images of (a) opaque BC film, (b) transparent *it*-PP film and (c) BC/*it*-PP composite film. (d) Transmittance of BC, *it*-PP, and BC/*it*-PP films in the UV-visible wavelength region.

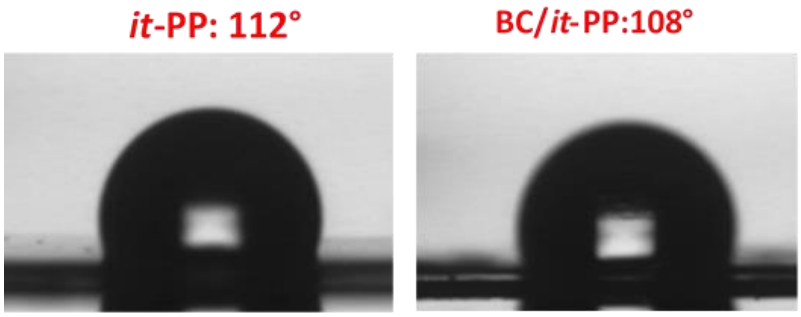

Figure 3-9. Contact angles of *it*-PP and BC/*it*-PP films on their surfaces.

The contact angles of *it*-PP and BC/*it*-PP films were exhibited in Figure 3-9. The BC/*it*-PP composite film showed a contact angle of 108 °, which was close to that of neat *it*-PP film. The sandwich-like of BC/*it*-PP film should be the reason for the hydrophobicity enhancement.

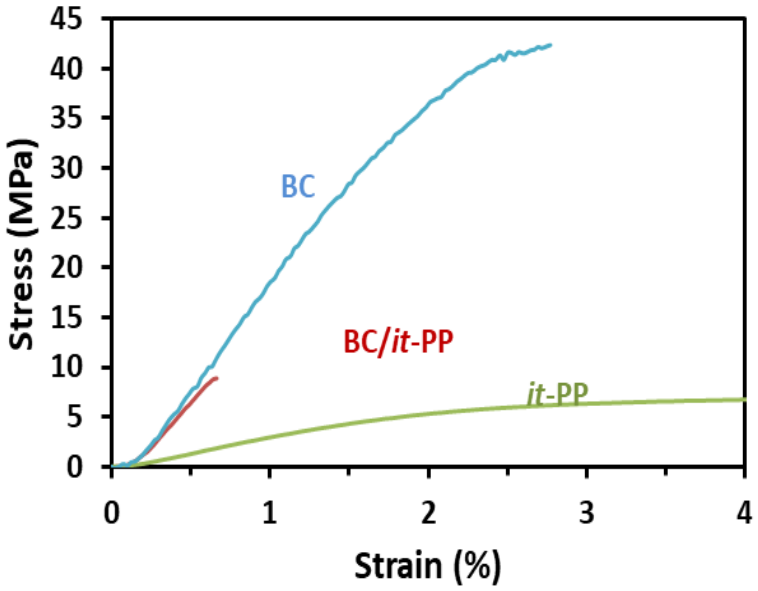

Figure 3-10. Tensile stress-strain curves for BC, *it*-PP and BC/*it*-PP films.

Table 3-2. Mechanical properties of BC, *it*-PP[a] and BC/*it*-PP films.

	Tensile strength (MPa)	Strain at break (%)
BC	42	2.7
it-PP	7.1	6.9
BC/*it*-PP	8.9	0.6

[a] For convenience, only part of the stress-strain curve of *it*-PP was exhibited

Typical tensile stress-strain curves of BC, *it*-PP and BC/*it*-PP films were shown in Figure 3-10, whereas data obtained from these tests can also be found in Table 3-2. The ultimate tensile strength of BC/*it*-PP (~8.9 MPa) was similar to that of *it*-PP film (~7.1 MPa), whereas the elongation of the composite film was much smaller than that of *it*-PP film. Therefore, the combination between BC and *it*-PP didn't improve the mechanical properties of *it*-PP film.

3.4 Conclusion

In this chapter, the author developed a novel composite film composed of BC and *at*-PP by a facile and cost-effective hot-press procedure, elucidating the changes in transparency, morphology, hydrophobicity and mechanical properties. The transparent BC/*at*-PP composite film showed a typical three-layer structure which led to the good hydrophobicity of the resulting film. It was revealed that the presence of BC matrix significantly enhanced the physical strength of *at*-PP film. Furthermore, the good thermal stability of the composite film was proved. As control, BC/*it*-PP composite film was also fabricated with the same method which exhibited unsatisfactory transparency and mechanical properties. In conclusion, the present BC/*at*-PP composite film is promising as transparent film for food packaging and optoelectronics applications.

3.5 References

1. R. Jung, H-S. Kim, Y. Kim, S-M. Kwon, HS. Lee, H-J. Jin, *J. Polym. Sci. Part B Polym. Phys.*, 2008, **46**, 1235-1242.
2. M. Nogi, S. Iwamoto, AN. Nakagaito, H. Yano, *Adv. Mater.*, 2009, **21**, 1595-1598.
3. H. Yano, J. Sugiyama, A.N. Nakagaito, M. Nogi, T. Matsuura, M. Hikita, K. Handa, *Adv. Mater.*, 2005, **17**, 153-155.
4. A. Putra, A. Kakugo, H. Furukawa, J.P. Gong, Y. Osada, *Polymer*, 2008, **49**, 1885-1891.
5. Z. Yan, S. Chen, H. Wang, B. Wang, J. Jiang, *Carbohydr. Polym.*, 2008, **74**, 659-665.
6. S.K. Padmanabhan, C.E. Corcione, R. Nisi, A. Maffezzoli, A. Licciulli, *Eur. Polym. J.*, 2017, **93**,192-199.
7. F. Quero, M. Nogi, H. Yano, K. Abdulsalami, S.M. Holmes, B. H. Sakakini, S. J. Eichhorn, *ACS Appl. Mater. Inter.*, 2009, **2(1)**, 321-330.
8. Z.Q. Li, Q. Jia, C.H. Pei, *Cellulose*, 2016, **23(4)**, 2449-2455.
9. S. Gea, E. Bilotti, C.T. Reynolds, N. Soykeabkeaw, T. Peijs, *Mater. Lett.*, 2010, **64(8)**, 901-904.
10. Z. Zhang, R. Zhang, Y. Huang, J. Lei, Y.H. Chen, J.H. Tang, Z.M. Li, *Ind. Eng. Chem. Res.*, 2014, **53(24)**, 10144-10154.
11. E.R.P Pinto, H.S. Barud, R.R. Silva, M. Palmieri, W.L. Polito , V.L. Calil, M. Cremona, S.J.L. Ribeirob, Y. Messaddeq, *J. Mater. Chem. C*, 2015, **3(44)**, 11581-11588.
12. A. Retegi, I. Algar, L. Martin, F. Altuna, P. Stefani, R. Zuluaga, P. Gañán, I. Mondragon, *Cellulose*, 2012, **19(1)**, 103-109.

13. M. Nogi, K. Handa, A.N. Nakagaito, H. Yano, *Appl. Phys. Lett.*, 2005, **87(24)**, 243110.

Concluding Remarks

In this doctoral thesis, bacterial cellulose-based functional composites with enhanced mechanical properties were developed. BC hydrogel possesses unique layered structure and thus can be used to prepare composite hydrogel with anisotropic stimuli-responsive property; BC aerogel exhibits excellent porous structure and low density. Converting its inherent hydrophilicity to hydrophobicity with other hydrophobized materials will ensure its potential application for oil/water separation; The pores of BC film can be easily filled with polymer resins and transparent BC-based composite film can be obtained. Such BC-based composites maintained the superior mechanical properties of BC while preserving the functional properties of the invading polymeric materials. The results obtained through this thesis are summarized as follows.

In Chapter 1, the preparation of MDI-modified BC/PNIPAAm composite hydrogels by in situ polymerization process and their unique thermo-sensitive properties are descripted. The MDI modification aimed to protect the layered structure of BC hydrogel. The influence of the molar ratio of MDI/glucose unit of BC on the morphology, mechanical properties and responsive rate to temperature were systematically explored. Furthermore, the anisotropic thermo-sensitivity of the composite hydrogel was revealed with the fact that the gel only swelled and deswelled perpendicular to the layers uniaxially, making the present composite hydrogel a promising choice in biomedical fields such as artificial muscles.

In Chapter 2, a novel MDI-modified BC/silica composite aerogel was prepared by a facile sol-gel process followed by freeze-drying and compared with pristine BC aerogel and BC/silica aerogel without modification. The resulting MDI-BC/silica aerogel exhibited excellent hydrophobicity due to the presence of hydrophobized silica

skeleton as well as MDI modification. The mechanical properties, shape-recovery capability, oil absorption ability and recyclability of the obtained composite aerogels were also investigated. As expected, the MDI-BC/silica composite aerogel showed superior mechanical properties, satisfactory oil absorption capability as well as desired recyclability, which were essential for ideal oil sorbent that can be utilized for oil/water separation.

In Chapter 3, a novel BC/*at*-PP composite film was fabricated *via* a facile and cost-effective "sandwich" hot-press method, during which the *at*-PP resin filled the porous structure of BC film and formed a dense film surface. BC/*at*-PP film with good transparency was thus obtained. With a typical three-layered structure, the present composite film exhibited good hydrophobicity which was beneficial to avoid or decrease the hygroscopicity of the film. The presence of BC nanofiber networks significantly enhanced the physical strength of *at*-PP film and the good thermal stability of the composite film was proved. Such BC/*at*-PP composite film holds tremendous potential as transparent film for food packaging and optoelectronics applications.

In conclusion, three types of functional composites were successfully prepared from BC and other functional materials. BC in different forms (hydrogel, aerogel and film) were used as matrix to prepared MDI-BC/PNIPAAm hydrogel, MDI-BC/silica aerogel and BC/*at*-PP film with high mechanical strength. With desired functional properties, these BC-based functional composites would find promising applications in various fields.

List of Publications

1. Rapid uniaxial actuation of layered bacterial cellulose/poly(*N*-isopropylacrylamide) composite hydrogel with high mechanical strength

   Qidong Wang, Taka-Aki Asoh and Hiroshi Uyama*

   RSC Advances, 2018, 8(23), 12608-12613.

2. Facile fabrication of flexible bacterial cellulose/silica composite aerogel for oil/water separation

   Qidong Wang, Taka-Aki Asoh*, and Hiroshi Uyama*

   Bulletin of the Chemical Society of Japan, 2018, 91(7), 1138-1140.

3. Facile preparation of a novel transparent composite film based on bacterial cellulose and atactic polypropylene

   Qidong Wang, Taka-Aki Asoh*, and Hiroshi Uyama*

   Bulletin of the Chemical Society of Japan, accepted

Acknowledgments

This study was carried out from 2015 to 2018 at the Department of Applied Chemistry, Graduate School of Engineering, Osaka University. On finishing the PhD course, I'm really grateful for the kind assistance and support from all members around me during the three years.

First and foremost, I would like to express my deepest gratitude to my supervisor, Prof. Hiroshi Uyama, for his continuous guidance and invaluable discussion on my research. I would not be able to finish my study smoothly without his timely advice and kind-hearted encouragement. I also sincerely thank him for giving me a chance to attend the 6th international conference on bio-based polymers held in Taiwan. His keen and vigorous academic observations enlighten me in my future study and career.

I am profoundly grateful to Associated Prof. Taka-aki Asoh, for his suggestions and inspirations to improve the quality of my research. I also thank him for his efforts in knowledge sharing and manuscripts revising. Without his help, this thesis would not be possible.

I appreciate Assistant Prof. Takashi Tsujimoto for his heartfelt supports and expert advice.

Special thanks to Ms. Yoko Uenishi, Ms. Tomoko Shimizu and Ms. Yoshimi Shinomiya for their kind help and warm-hearted support.

I am very thankful to the past and present fellow labmates in Uyama Lab: Dr. Yashushi Takeuchi, Dr. Boxing Zhang, Dr. Tengjiao Wang, Dr. Hyunhee Shim, Dr. Yu Shu, Dr. Tomonari Kanno, Ms. Zhaohang Yang, Mr. Chen Qian, Mr. Zhengtian Xie, Ms. Yankun Jia, Mr. Keng Yao Tan, Ms. Jingyuan Niu, Ms. Xingyu Xiang, Ms. Jin Qian, Ms.

Yiying Wang, Mr. Haoyan Zhou, etc. for their kind-hearted help both in my research and daily life.

The financial support from China Scholarship Council (CSC) for my academic study and my stay in Japan is greatly appreciated.

Finally, I would like to express particular appreciation to my parents and Ms. Mengyan Wang, Mr. Zuoyong Gong and Mr. Qimeng Wang for their endless support and love throughout my life. The warm encouragement from my family motivates me to persist in my research and study.

July 2018

Qidong Wang